Geological Quarterly, 2007, **51** (4): 453–476

Conodont biostratigraphy of the Frasnian–Famennian boundary in the Esfahan and Tabas areas, Central Iran

Hossein GHOLAMALIAN

Gholamalian H. (2007) — Conodont biostratigraphy of the Frasnian–Famennian boundary in the Esfahan and Tabas areas, Central Iran. Geol. Quart., **51** (4): 453–476. Warszawa.

The Frasnian–Famennian (F–F) boundary in Central Iran has been investigated on the basis of conodont faunas (34 species and subspecies) from four sections: Chahriseh near Esfahan, and Kal-e-Sardar, Howz-e-Dorah and Ghale-Kalaghu near Tabas. The F–F boundary in the Chahriseh section is located in a one-metre interval between beds EX1 and F-F9 whereas in the Kal-e-Sardar section it is at the base of bed Cly1. The F–F boundary cannot be recognized in the Howz-e-Dorah and Ghale-Kalaghu sections because of unconformable relationships and erosion of the uppermost late Frasnian beds indicated incidentally by reworked boulders (indicating contemporaneous tectonic activity) and by the abrupt appearance of contrasting environments, including tempestites at the base of the lower Famennian. The best conodont and palaeoenvironmental data were obtained from the Kal-e-Sardar section where a deeper marine environment prevailed during the late Frasnian, becoming shallower in the early Famennian; the Chahriseh section displays small fluctuations in sea level during the early Famennian. The conodont faunas display the inception of the *Polygnathus communis* group in the late Frasnian (*rhenana–linguiformis* zones) and the appearance of *Icriodus alternatus mawsonae* in the Late *rhenana* Zone. A new age-range is suggested for *Polygnathus aequalis* Klapper and Lane, from the *transitans* to the *linguiformis* zones. Three conodont biozones are represented in the late Frasnian to early Famennian of the Chahriseh section, two late Frasnian and one early Famennian in the Kal-e-Sardar section and two biozones in the late Frasnian and early Famennian of both the Howz-e-Dorah and Ghale-Kalaghu sections. Two new species are described: *Polygnathus tabasianus* (Early to Late *crepida* zones) and *Polygnathus vachiki* (Late *rhenana–linguiformis* zones).

Hossein Gholamalian, Department of Geology, Faculty of Sciences, Hormozgan University, Po. Box 3995, Bandar Abbas, Iran; e-mail: h_gholam@yahoo.com (received: February 8, 2006; accepted: March 27, 2007).

Key words: Iran, Late Devonian, Frasnian–Famennian boundary, biostratigraphy, conodonts.

INTRODUCTION

The Global Stratotype Section and Point (GSSP) for the Frasnian–Famennian (F–F) boundary is designated at Coumiac in the Montagne Noire of southern France (Klapper *et al*., 1993; House *et al*., 2000). High-precision identification of this boundary is best based on conodonts and sometimes on ammonoids.

The mass extinction event associated with that boundary (Upper Kellwasser Event: e.g. McGhee, 1996) has been studied by numerous researchers notably by Sandberg *et al.* (1988) and Ziegler and Sandberg (1990). Their zonation through this interval has been based primarily on marine pelagic genera, especially *Palmatolepis*, a genus that is generally very rare or absent from Iranian sequences. Faunas studied for the purpose of this paper are from obviously shallower marine biofacies than the sequences that provided the basis for the Late Devonian zonations. That notwithstanding, both presently utilized zonal schemes (Klapper, 1989; Ziegler and Sandberg, 1990) and the Frasnian–Famennian boundary can be applied with reasonable accuracy in the Iranian successions.

Exemplary studies of the F–F boundary, apart from the now classic Coumiac sequence, have been undertaken in various countries in Europe, North America, north Africa and east Asia (e.g. Morrow, 2000; Racki and House, 2002; Racki, 2005). Chen *et al*. (2005) described the F–F crisis on the basis of analyses of ^{13}C and $^{87}Sr/^{86}Sr$ in some sections of southern China. Racki and Baliński (1998) documented brachiopods across the boundary in southern Poland. Yazdi (1999) suggested location of the F–F boundary in a terrigenous interval in the southern Shotori Range of eastern Iran, but this was based on a single broken conodont element that appears to have been re-worked. Subsequent data indicates that the uppermost Frasnian is absent in the southern Shotori Range, having been removed by erosion.

Dastanpour and Aftabi (2000) have presented preliminary isotopic data from across the F–F boundary in the Kerman region of southeastern Iran, and Mahmudy Gharaie *et al*. (2003, 2004) have undertaken a reconnaissance study of sedimentation and

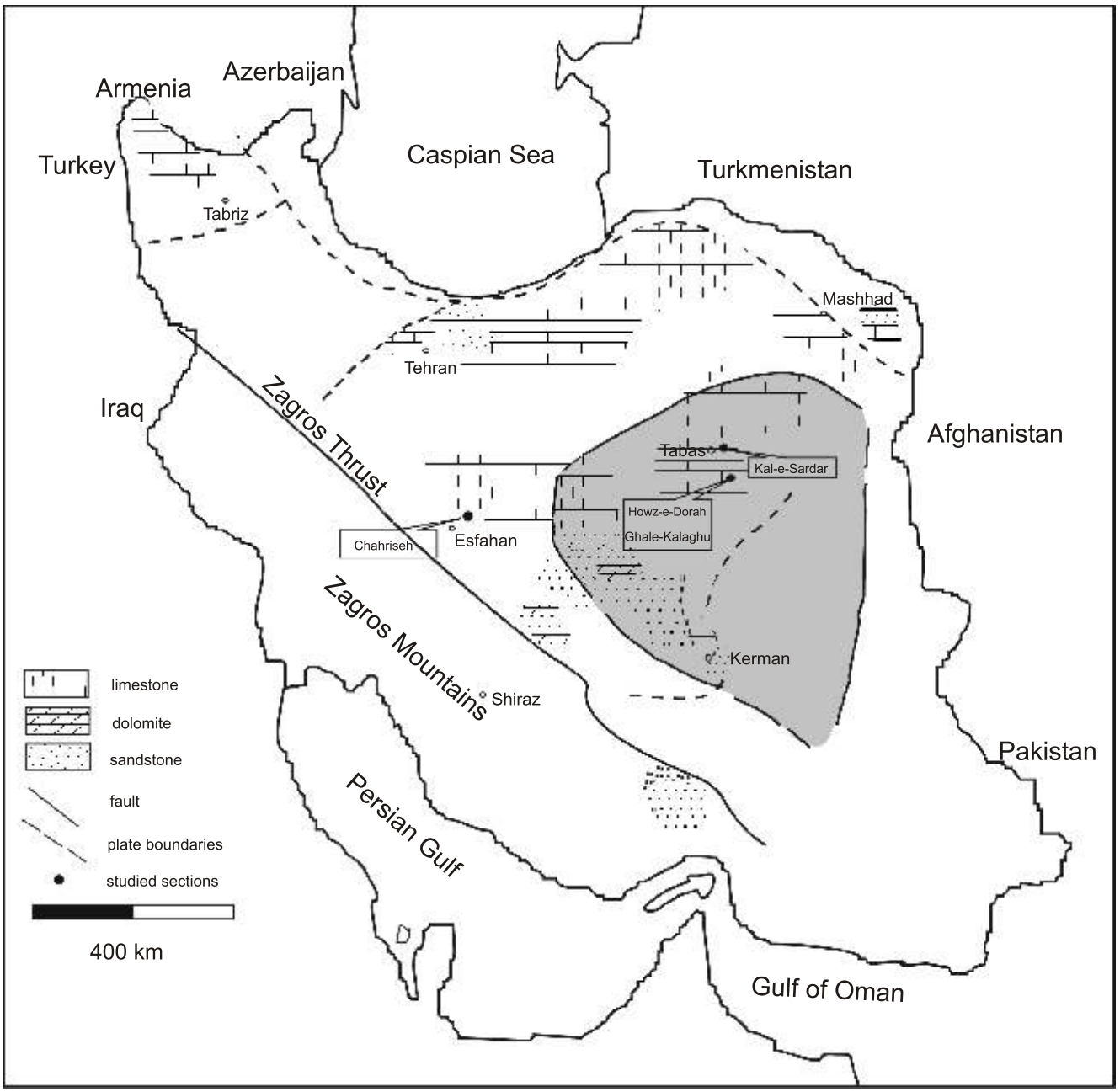

Fig. 1. Late Devonian palaeogeographic map of Iran and location of the studied sections

The map is redrawn from Wendt *et al*. (2005); the shaded area is the East-Central Iran microplate

isotope chemistry across the F–F boundary in Central Iran. Both studies, unfortunately, were not tied to high resolution biostratigraphic data. In the present study, more precise information on the Upper Kellwasser Extinction Event in Iran and on the conodont biostratigraphy across the F–F boundary is given.

Wendt *et al*. (2002) identified the Frasnian–Famennian boundary in some southeastern sections of Iran such as Hutk, but this identification is based on poor samples which do not contain any index species. These authors recently examined many sections of Central, Southeastern and Northern Iran and identified the F–F boundary in some of them such as Khoshyeilagh, Howz-e-Dorah, Niaz, Anarak and Kuh-e-Kanseh based on lithofacies changes and poor fossil collections (Wendt *et al*., 2005), but more precise and high resolution biostratigraphic data on the Frasnian–Famennian boundary are still needed.

Four sections (Figs. 1 and 2) were chosen for study: the Kal-e-Sardar section in the middle of the Shotori Range near the Sardar River, 23 km east of Tabas; the Chahriseh section 10 km east of the Esfahan–Ardestan road, 55 km north-east of Esfahan (Fig. 3); and the Howz-e-Dorah and Ghale-Kalaghu sections, 500 m apart near the Chiruk mine in the southern Shotori Range, 70 km south of Tabas (Fig. 4). Leaching of 152 limestone samples from these sections in acetic acid produced 3841 conodont elements ascribed to 34 species and subspecies of conodonts (in 6 genera) from 56 productive samples.

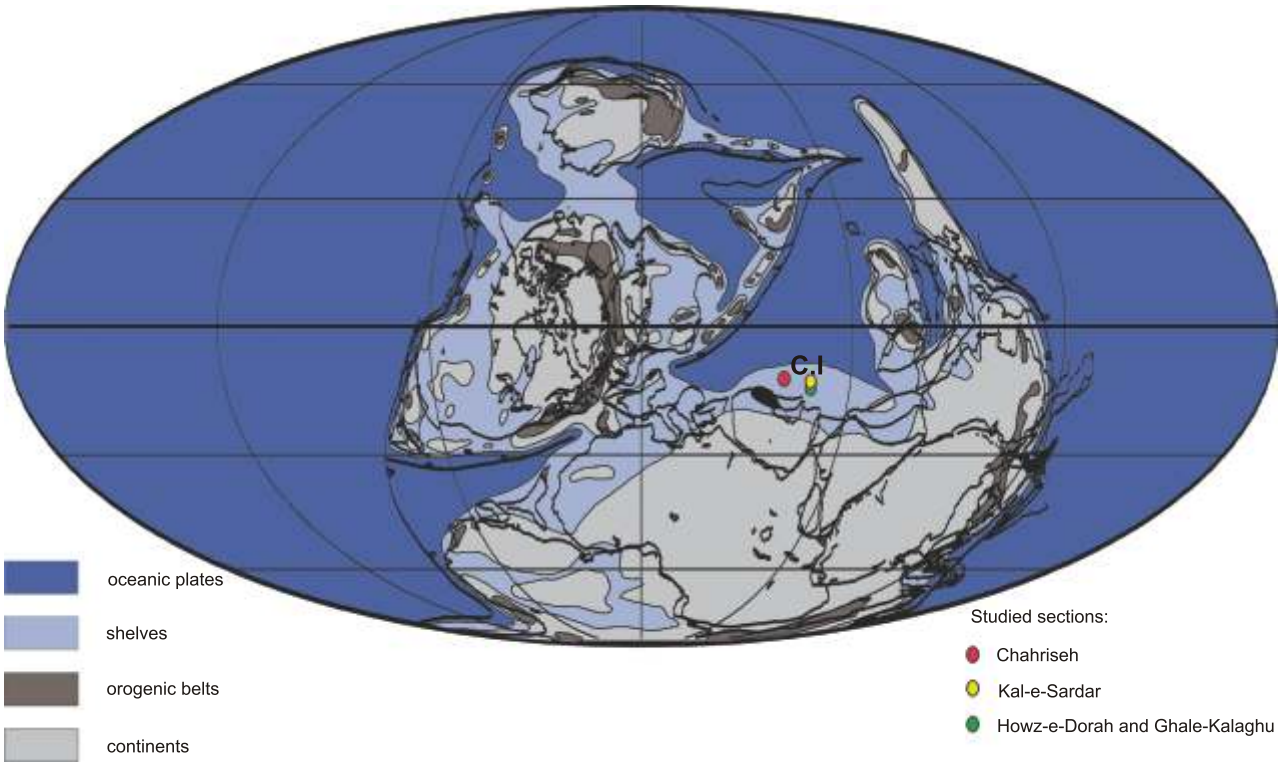

Fig. 2. Late Devonian global palaeogeographic map and location of sections

C.I = Central Iran; the background is based on Golonka *et al*. (1994)

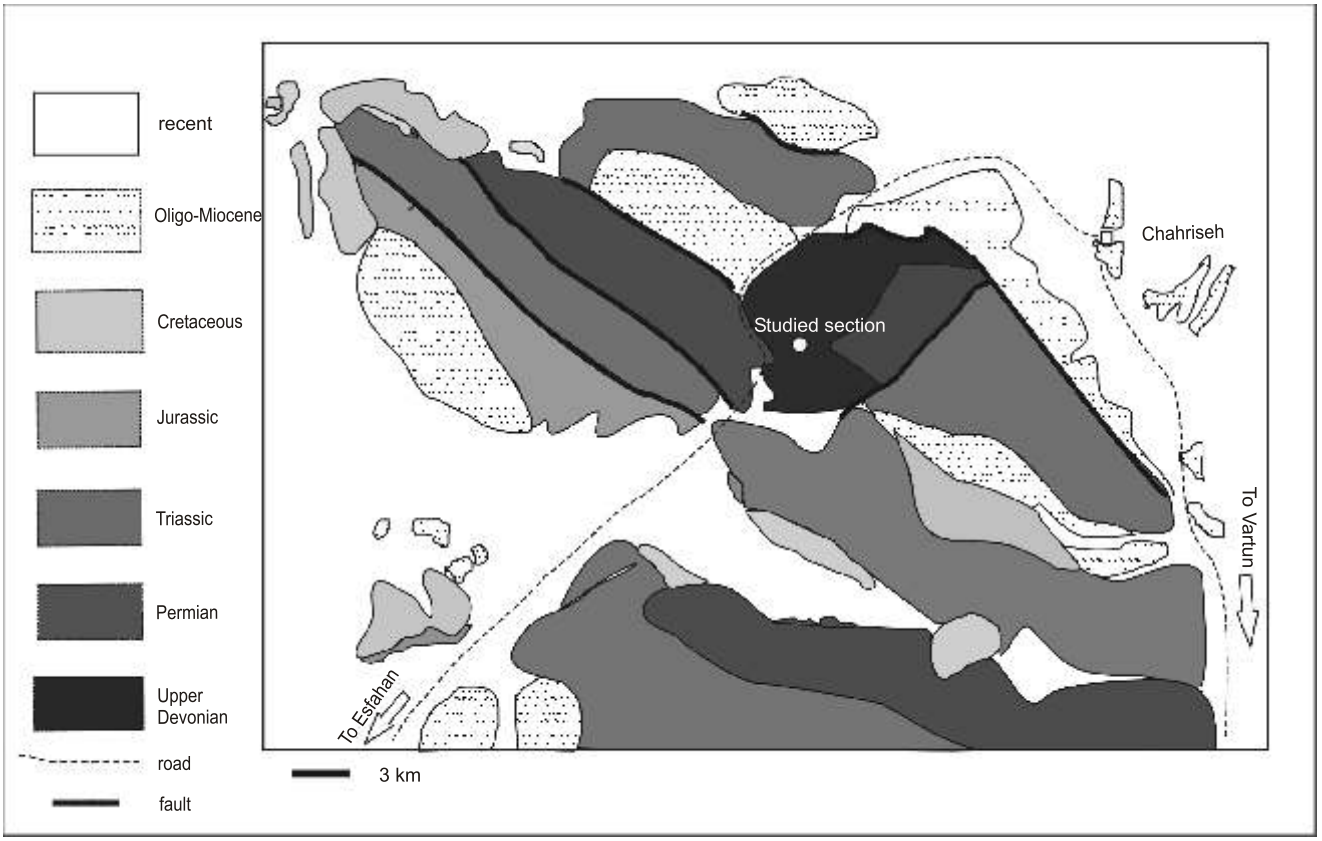

Fig. 3. Geological map of the Chahriseh area (Yazdi *et al.*, 2000)

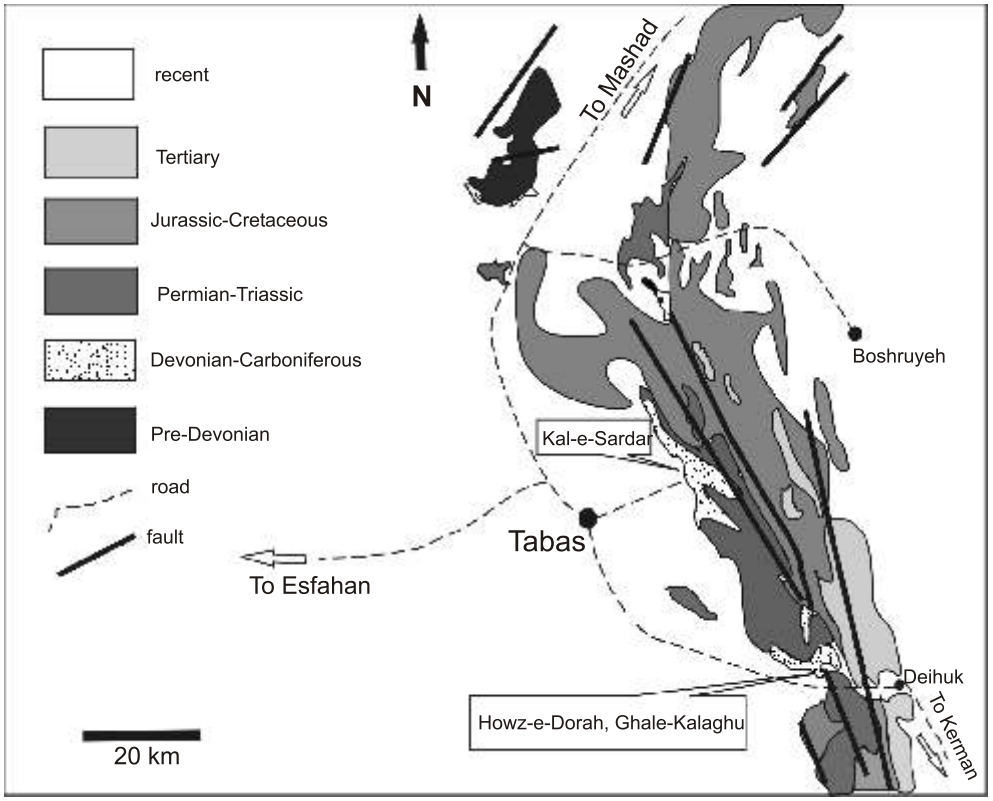

Fig. 4. Geological map of the Tabas area by Stöcklin *et al*. (1965)

UPPER DEVONIAN OF CENTRAL IRAN

Two sedimentary formations are represented in the Upper Devonian of Central Iran, the Bahram and Shishtu formations. The Bahram Formation consists of 300 m of limestones with brachiopods, corals and stromatoporoids regarded as Givetian to Frasnian by Stöcklin and Setudehnia (1991). They pointed out that equivalent sequences can be observed in many parts of Iran, e.g. in Esfahan, Kerman, Shirgesht and the Shotori Range. Member 2 of the Bahram Formation shows an abundance of colonial rugose corals, stromatoporoids and tabulate corals; it has been referred to the Frasnian (Rohart, 1999; Mistiaen *et al.*, 2000). Brice *et al*. (1999), who studied the distribution of brachiopods and other biota in Eastern and Central Iran, stressed the disappearance of reef-building fossils at the top of the Bahram Formation (and equivalent strata) as reflecting the first step in the latest Frasnian mass extinctions, suggesting correlation with the Lower Kellwasser Event.

The Shishtu Formation has been divided into two members with the F–F boundary being located in Shishtu 1.

The names (Bahram and Shishtu formations) were introduced in an unpublished manuscript by Ruttner *et al.* (1965) but were not formalised until three years later (Ruttner *et al*., 1968). They divided both formations into two members, Bahram 1 and Bahram 2, and Shishtu 1 and Shishtu 2. Stöcklin *et al.* (1965) studied the Shishtu Formation in the Shotori Range and proposed some sections near Howz-e-Dorah (Howz-e-Dorah and Ghale-Kalaghu sections of this paper) and Kal-e-Sardar as reference sections. According to them, this formation is Frasnian to early Viséan in age. Yazdi (1999) was of similar opinion, though Ashouri (1990) believed its age to span a slightly shorter interval, Frasnian to late Tournaisian. Palynomorph study of Shishtu Formation in the Ozbak-Kuh Mountains (Hashemi and Playford, 1998) suggested a shorter age for the formation in that area: Frasnian to Famennian. A preliminary study of Late Devonian cephalopods has been undertaken by Walliser (1966).

CHAHRISEH SECTION

The lower part of this section in West-Central Iran is mostly sandstone and dolostone with palynological data suggesting a Frasnian to Famennian age (Ghavidel-Syooki, 2001). Vertebrate micro-remains and a few conodonts from beds near the base of the section (Turner *et al*., 2002) have not included the zonally important index conodont species specified by Ziegler and Sandberg (2000) that might indicate the middle *falsiovalis* to Late *hassi* zones (Turner *et al.*, 2002). According to Turner (1997) and Valiukevicius (1998), abundant microvertebtrate remains (*Australolepis seddoni* and *Nostolepis* cf. *goujensis*) confirm an early Frasnian age for the base of the section (*cf*. Turner *et al*., 2002). This part is equivalent to Bahram 1.

The upper part of the section, consisting of carbonates with a diverse epifauna including biostromes with rugose and tabulate corals and stromatoporids, has been regarded as Givetian to late Frasnian in age (Mistiaen *et al*., 2000; Mistiaen and Gholamalian, 2000; Rohart, 2000), though brachiopods from the biostromes were regarded as mid-Frasnian (Jafarian, 2000; Brice

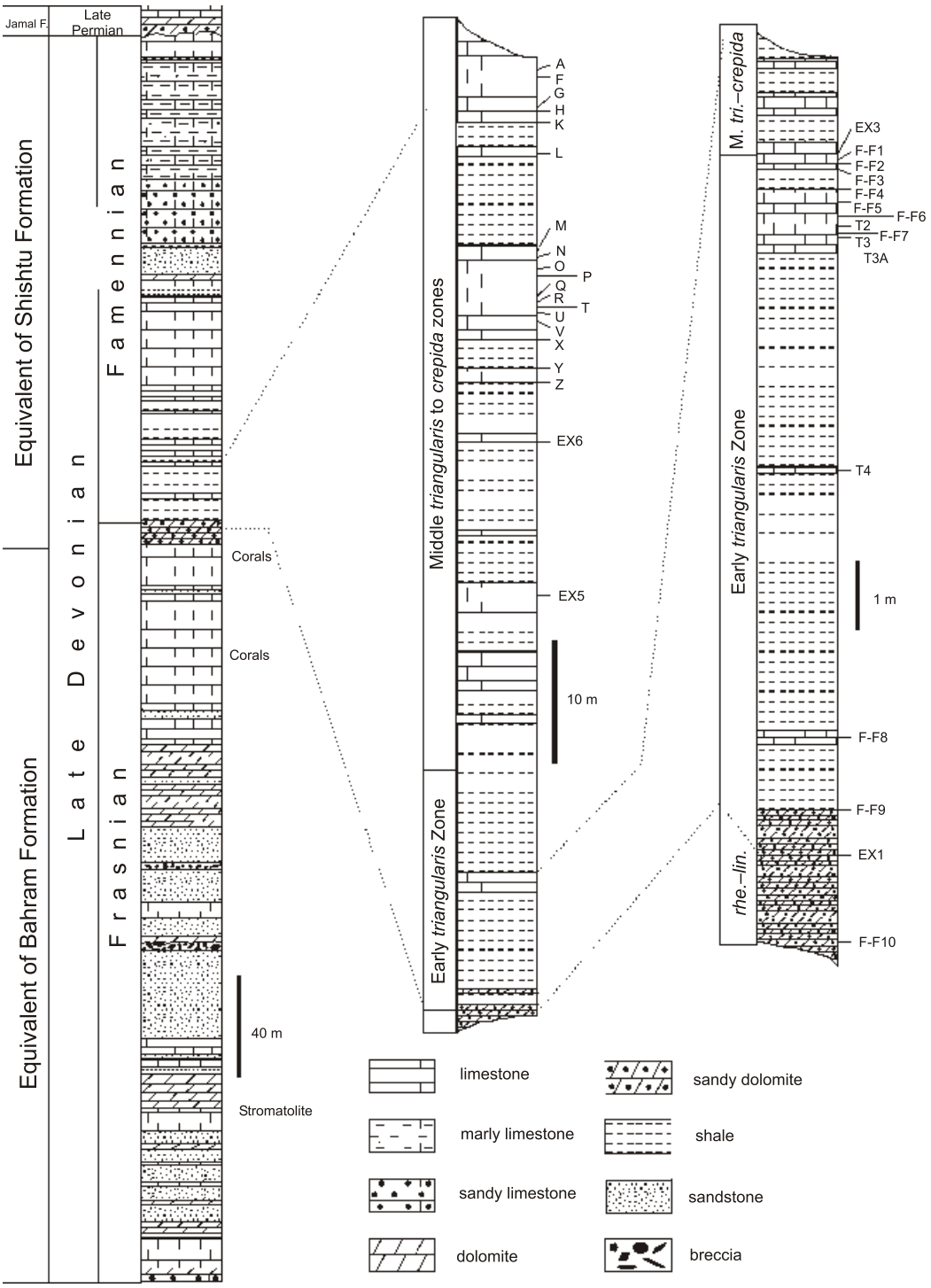

Fig. 5. Stratigraphic column of the Chahriseh section, the column has been closed up two times to show detailed lithology and sampling

M — middle, *tri.*— *triangularis*, *rhe.* — *rhenana*, *lin.*— *linguiformis*

and Kebria-ee, 2000). This unit is equivalent to Bahram 2. Limestones and marly limestones at the top of sequence were assumed to be Famennian in age. Late Frasnian and Famennian beds correspond to Shishtu 1. Conodont-based investigations (Gholamalian, 1998, 1999, 2003) indicated a Frasnian to late Famennian age for the section as a whole. Data now presented accords with the position of the Frasnian–Famennian boundary as being within the one-metre interval between the top of sample EX1 and the base of sample F-F9, lower than assumed in previous papers (Fig. 5).

KAL-E-SARDAR SECTION

Stöcklin *et al*. (1965) were the first to examine the numerous and discontinuous outcrops of Shishtu Formation at Kal-e-Sardar and attribute a Late Devonian age to them. The

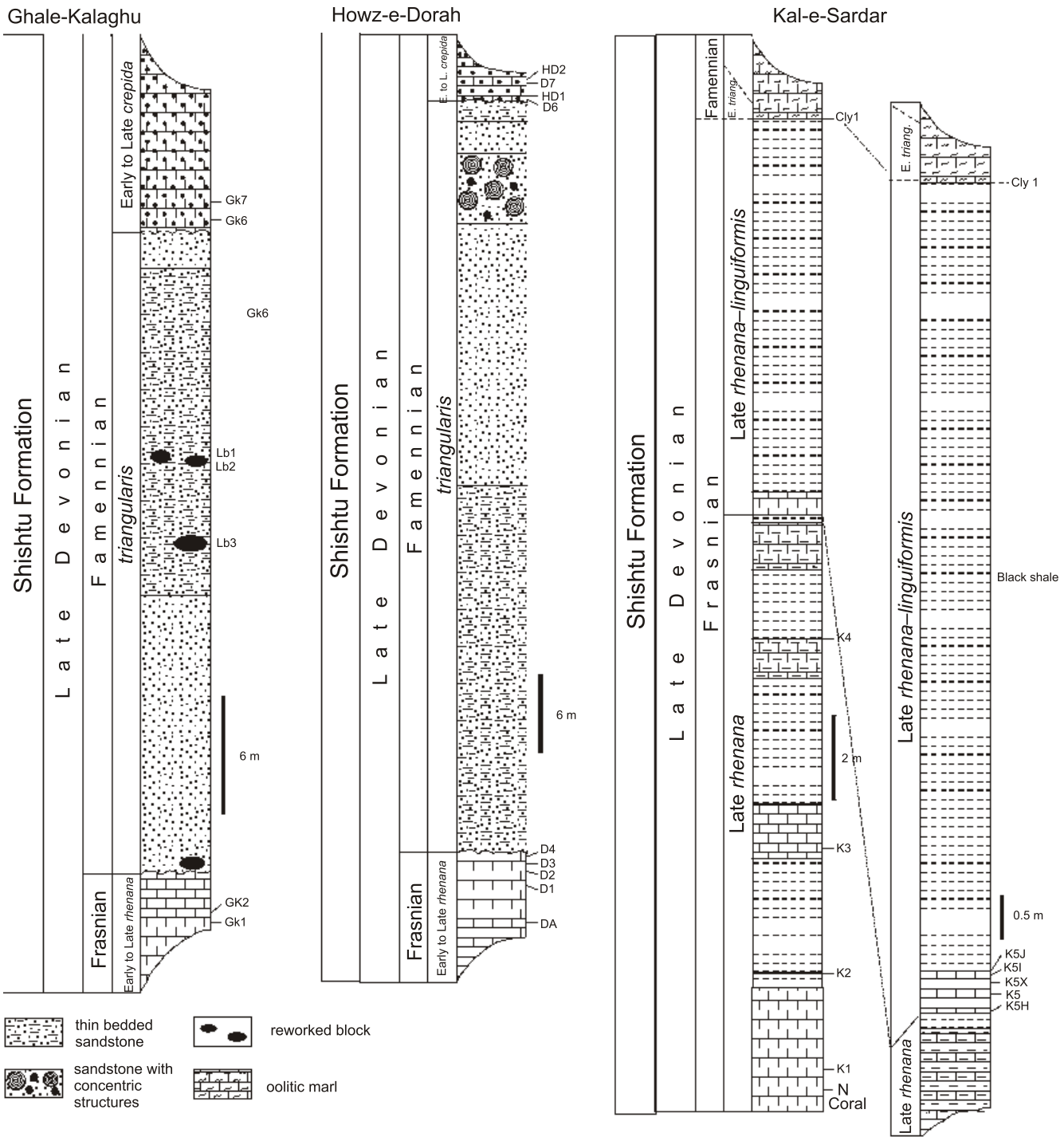

Fig. 6. Stratigraphic columns and sampling of the Kal-e-Sardar, Howz-e-Dorah and Ghale Kalaghu sections

Samples from reworked blocks are shown as Lb1 and Lb3; E. — Early, L. — Late; other explanations as in Figure 5

F–F boundary is located in the Shishtu 1 member. The most continuous sequence, studied in the present investigation, differs in fauna and lithology from the southernmost Shishtu sections in the southern Shotori Range (see below). Its base is a bed rich in late Frasnian rugose corals and conodonts. Higher in the sequence is a bed of oolitic limestone with cephalopods (Fig. 6) but, unfortunately, it has proved barren of conodonts. Reworked boulders in the Ghale-Kalaghu section, stratigraphically and lithologically very similar to this horizon, may have been derived from it.

Some late Frasnian and mid-Famennian beds of this area, rich in cephalopods, were not encountered in the southern Shotori Range sections.

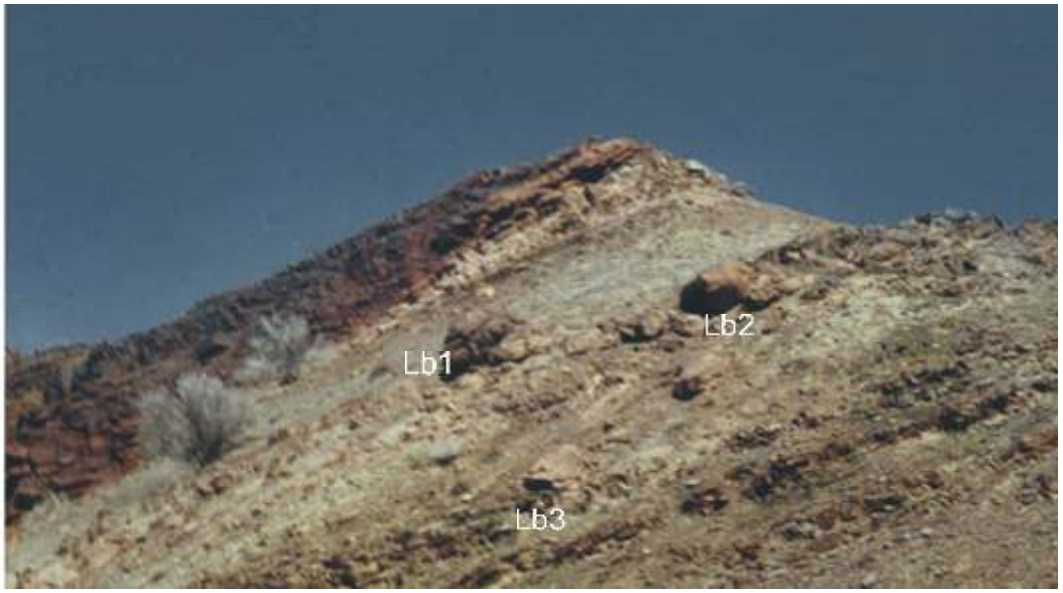

Fig. 7. Ghale-Kalaghu section, reworked boulders (Lb1, Lb2 and Lb3) are scattered in the laminar sandstone beds

Some marly limestones in the middle of the section are very rich in late Frasnian conodonts (Fig. 6). According to Yazdi (1996) these beds contain the cephalopod *Beloceras* and were therefore named the "*Beloceras* beds". Yazdi (1999) has studied conodonts and cephalopods from richly fossiliferous marly beds at the top of sequence-dated herein as mid-Famennian (Late *marginifera* Zone). Becker *et al*. (2004) studied the cephalopod fauna in the middle of the marly beds, assuming it represented the *Annulata* Event (Late *trachytera* Zone), but conodont data presented here indicate the base of this interval to be early Famennian (Early *triangularis* Zone). Barren black shale (8.7 m) between these fossiliferous late Frasnian and early Famennian lithological packages, and the presence of *Palmatolepis triangularis* immediately above this interval, accords with all of the black shale package being regarded as most likely late Frasnian (Late *rhenana* to *linguiformis* zones). The section studied is a part of one of the Shishtu Formation reference sections (Shishtu 1). The Kal-e-Sardar section of the present study is located on Hill IV of Becker *et al*. (2004) and underlies their section. Because of its position near the Naiband fault in the western flange of the Shotori Range, the Shishtu Formation is fragmented, but Hill IV is not affected.

HOWZ-E-DORAH AND GHALE-KALAGHU SECTIONS

Howz-e-Dorah and Ghale-Kalaghu are two reference sections of the Shishtu Formation in the southern Shotori Range (Stöcklin *et al*., 1965). Both section can be divided into two members and the Frasnian–Famennian boundary is located in Shishtu 1. Yazdi (1999) studied a complete section of the Shishtu Formation at Howz-e-Dorah where he estimated a total thickness of 570.5 m. An interval of 71.5 m, commencing with yellow limestones with large placoderm plates identified as *Aspidichthys*, referred to as the "placoderm beds" (Yazdi *et al*., 1999) was chosen for study (Fig. 6). Yazdi (1999, 2000) assigned these beds to the *linguiformis* Zone, suggesting the F–F boundary to be in the middle of an interval of laminar sandstones. New conodont data indicate the Early to Late *rhenana* zones for the placoderm-bearing beds. There are two disconformities: one at the base and a second at the top of the laminar sandstone beds. The top of the late Frasnian succession and the erosion surface can be observed in the field; the Upper Kellwasser equivalents could not be recognized. The upper disconformity surface has also been shown by Wendt *et al*. (2005, pl. 3, figs. 2 and 3) and they have proposed this level as the Frasnian–Famennian boundary. Mahmudy Gharaie *et al*. (2004) followed Yazdi *et al*. (1999) concerning the location of the boundary.

The Ghale-Kalaghu section is very similar to the Howz-e-Dorah section, but with a few reworked limestone boulders (with Early *rhenana* to *linguiformis* zones conodonts) scattered through a matrix of laminar sandstones (Fig. 7). Similar occurrences are known from other areas, e.g. late Frasnian reefal blocks transported by debris flows into Late Devonian carbonates in the Canning Basin (Australia; Becker *et al*., 1991).

The Iranian blocks are diverse in lithology and inferred environments: oolitic limestone and white sandstone. Fragments of fossil wood material in the latter may suggest a non-marine environment, though it is well-known that plant material can be transported. The lithology and the associated unconformities above and below the laminar sandstone interval, are considered to correspond to a major regression during the early Famennian (e.g. Sandberg *et al*., 1988) in the southern Shotori Range associated with tectonic activity, subaerial exposure, erosion of the top of the late Frasnian sequence and an important interval of clastic sedimentation. According to Mahmudy Gharaie *et al.* (2004) the climate around the F–F boundary was humid and warm. The sandstone succession in both of the Howz-e-Dorah and Ghale-Kalaghu sections is capped by a disconformity surface, overlain by red sandy limestone. The latter has produced conodont faunas indicative of the Early to Late *crepida* zones.

BIOSTRATIGRAPHY

This work is based on 152 samples acid-leached from four stratigraphic sections; 56 of them produced conodonts ascribed to 34 species and subspecies of six genera. Abbreviations used: *Ad.* — *Ancyrodella*, *Ag.* — *Ancyrognathus*, *I.* — *Icriodus*, *Pal.* — *Palmatolepis*, *Pel.* — *Pelekysgnathus*, *P.* — *Polygnathus*.

CHAHRISEH SECTION

Thirteen conodont species and subspecies from the Chahriseh section indicate that three biostratigraphic intervals can be discriminated (Fig. 5; Table 1).

Early *rhenana* to *linguiformis* zones. This interval is identified by the presence of *Icriodus alternatus alternatus*, *I.* sp., *Polygnathus politus*, *P. evidens* and *P.* sp. B. Among associated conodonts are *P. brevilaminus* and the *P. communis* group.

Early *triangularis* Zone. *I. iowaensis iowaensis*, *Pel. serradentatus*, *I. alternatus alternatus* and *I.* aff. *I. cornutus* occur in this interval associated with the *P. communis* group as well as with *P. brevilaminus*, *P.* sp. A and *P.* sp. B. There is no sign of any zonal or index conodont in this interval but the stratigraphic situation helps us to attribute this strata to the Early *triangularis* Zone. *Pel. serradentatus* ranges from the *triangularis* to the *crepida* zones (Capkinoglu, 1991; Capkinoglu and Gedik, 2000). However, a one-metre barren zone intervenes between the lowest sample attributable to Early *triangularis* Zone and the uppermost bed attributable to Early *rhenana* to *linguiformis* zones preventing a high-precision location of the F–F boundary.

Middle *triangularis* to *crepida* zones. Characteristic of this interval are *I. iowaensis iowaensis*, *I.* aff. *I. cornutus* and *I. multicostatus multicostatus*. Among associates are *I. alternatus alternatus*, *Pel. serradentatus*, *P. communis* group and *P. brevilaminus*. The lower boundary of this interval is identified by the appearance of *I. multicostatus multicostatus* in sample EX5 (Table 1).

KAL-E-SARDAR

The Kal-e-Sardar sequence produced 23 conodont species enabling discrimination of three biozones (Table 2).

Late *rhenana* Zone. *I. alternatus alternatus*, *I. alternatus mawsonae*, *Pal.* sp. A, *Ad. curvata*, *Ad. buckeyensis*, *Ag. triangularis*,

Table 1

Distribution chart of conodonts in the Chahriseh section

Zones	E. *rhe.–lin.*		Early *triangularis*														Middle *triangularis* to *crepida*														
Samples	F-F10	EX1	F-F9	F-F8	T4	T3A	T3	F-F7	T2	F-F6	F-F5	F-F4	F-F3	F-F2	F-F1	EX3	EX5	EX6	Z	Y	X	V	R	Q	P	O	N	M	L	K	H	G	A
Icriodus al. alternatus	1	3	2	1	10	42	4	1	2	4	4	8	3	1	2	1	4	6	1	12	4	2	–	12	4	4	2	19	–	–	–	1	–
I. aff. *I. cornutus*	–	–	–	–	6	14	–	–	–	–	–	–	–	–	1	4	–	5	1	20	–	–	4	1	–	–	–	17	–	–	–	–	–
I. iowaensis iowaensis	–	–	–	–	1	2	2	1	–	–	2	2	1	1	1	1	3	1	–	2	–	–	–	13	5	–	4	3	1	2	–	–	–
I. m. multicostatus	–	–	–	–	–	–	–	–	–	–	–	–	–	–	–	–	1	2	–	2	1	–	–	–	–	–	–	–	–	–	1	–	–
I. sp.	–	–	–	–	–	2	–	–	–	–	–	–	–	–	–	–	–	–	–	–	–	–	–	–	–	–	–	–	–	–	–	–	–
Polygnathus brevilaminus	5	–	–	1	3	47	–	–	–	–	1	1	2	4	–	–	–	–	–	1	–	–	–	–	–	–	–	–	–	–	–	–	–
P. communis group	4	–	–	–	1	14	1	1	–	–	–	7	7	2	1	12	3	3	1	6	4	2	–	5	1	5	2	6	–	–	1	1	1
P. evidens	–	2	–	–	–	–	–	–	–	–	–	–	–	–	–	–	–	–	–	–	–	–	–	–	–	–	–	–	–	–	–	–	–
P. politus	2	1	–	–	–	–	–	–	–	–	–	–	–	–	–	–	–	–	–	–	–	–	–	–	–	–	–	–	–	–	–	–	–
P. sp. A	–	–	–	–	–	3	–	–	–	–	–	–	–	–	–	–	–	–	–	–	–	–	–	–	–	–	–	–	–	–	–	–	–
P. sp. B	2	1	3	–	1	3	–	–	–	–	–	–	–	–	–	–	–	–	–	–	–	–	–	–	–	–	–	–	–	–	–	–	–
Pelekysgnathus sp.	–	–	–	–	1	3	–	–	–	–	–	2	–	–1	2	–	–	–	–	3	–	–	–	2	–	–	–	1	–	–	1	–	2
Pel. serradentatus	–	–	1	–	–	7	–	2	1	–	2	1	1	–	1	2	–	–	–	–	–	–	–	–	–	–	1	–	–	–	–	–	–
Unassigned elements	3	2	3	–	18	245	–	13	5	15	10	13	5	9	20	13	6	16	2	25	15	9	3	19	3	3	5	55	7	5	5	–	–
Total	17	9	9	2	41	382	7	18	8	19	20	33	19	18	28	31	16	33	5	71	24	13	7	52	13	12	14	101	8	7	8	2	3
Biofacies	P	–	–	–	I-P	P-I	–	I-P	–	I-P	I-P	I-P	P-I	P-I	I-P	P-I	I-P	I-P	–	I-P	I-P	–	–	I-P	–	–	–	I-P	–	–	–	–	–

E. — Early, *rhe.* — *rhenana*, *lin.* — *linguiformis*, *al.* — *alternatus*, *m.* — *multicostatus*, P — polygnathid, P-I — polygnathid-icriodid, I-P — icriodid-polygnathid

Table 2

Distribution chart of conodont species in the Kal-e-Sardar section, east of Tabas

Zones	L. *rhe.*	Late *rhenana–linguiformis*					E. *tri.*
Samples	N	K5H	K5	K5X	K5I	K5J	Cly1
Ancyrodella curvata	8	–	–	1	–	–	–
Ad. buckeyensis	1	8	12	3	–	–	–
Ancyrognathus triangularis	4	22	31	3	–	–	–
Icriodus alternatus alternatus	10	30	50	8	–	–	87
I. alternatus helmsi	–	10	15	–	–	–	1
I. alternatus mawsonae	4	6	10	–	–	–	24
I. xenium	–	–	1	–	–	–	–
Palmatolepis sp. A	1	2	1	–	–	–	–
Pal. winchelli	–	3	6	–	1	–	–
Pal. gigas gigas	–	2	4	–	–	–	–
Pal. aff. *Pal. perlobata*	–	–	–	–	–	–	15
Pal. sp. B	–	4	3	–	1	–	–
Polygnathus aequalis	–	24	7	–	2	2	–
P. brevilaminus	–	1	3	–	–	–	16
P. evidens	5	26	74	42	–	1	–
P. cf. *P. webbi*	–	–	–	–	–	–	19
P. politus	8	205	239	4	–	–	–
P. procerus	–	116	185	20	–	–	–
P. sp. B	–	12	3	–	–	–	–
P. sp. C	–	–	1	–	–	–	–
P. tenellus	–	–	–	–	–	–	18
P. vachiki n. sp.	–	2	8	4	–	–	–
P. webbi	3	17	24	21	1	–	–
Unassigned elements	31	287	410	60	1	2	47
Total	75	777	1087	166	6	5	227
Biofacies	P-I	P	P	P	–	–	I-P

L. — Late; *tri.* — *triangularis*; other explanations as in Table 1

P. evidens, *P. politus* and *P. webbi* occur in this biozone; it includes the oldest occurrence of *I. alternatus mawsonae*. Noteworthy in this interval is a richly fossiliferous bed with corals overlain by a metre of dark ferruginous oolitic limestone (with cephalopods).

Late *rhenana* to *linguiformis* zones. This interval is characterized by an association of *I. alternatus alternatus*, *I. alternatus helmsi*, *I. alternatus mawsonae*, *I. xenium*, *Ancyrodella curvata*, *Ad. buckeyensis*, *Ag. triangularis*, *Pal.* sp. A, *Pal. winchelli*, *P. aequalis*, *P. evidens*, *P. politus*, *P. procerus* and *P. webbi*. Other associated species are *P. brevilaminus*, *P. vachiki* n. sp., *Pal.* sp. B, *P.* sp. B and *P.* sp. C. Diagnostic of this biozone is *Pal. winchelli*. This assemblage Zone is comparable to zones 12 to13 of Klapper (1989). Some beds in this interval (K5 and K5H) are prolific in conodonts, suggesting especially favourable conditions for preservation.

Early *triangularis* Zone. An assemblage of *Pal.* aff. *Pal. perlobata*, *I. alternatus alternatus*, *I. alternatus mawsonae*, *I. alternatus helmsi*, *P. tenellus*, *P.* cf. *P. webbi* and *P. brevilaminus* occurs in this interval.

HOWZ-E-DORAH

Two biozones with 13 species and subspecies are recognized in this section (Table 3).

Early to Late *rhenana* zones. *I. alternatus alternatus*, *Ad. curvata*, *Ag. asymmetricus*, *P. aequalis*, *P. evidens*, *P. politus* and *P. webbi* occur in this interval. The placoderm bed of Yazdi *et al.* (1999) occurs in this biozone.

Early to Late *crepida* zones. *I. alternatus alternatus*, *Pal.* sp. aff. *Pal. perlobata* and *Pal. wolskajae* occur in this biozone. Co-occurring are *P. tabasianus* n. sp. and *P. brevilaminus*.

Wendt *et al.* (2005) proposed the range of *triangularis*–Early *crepida* zones for these strata. Yazdi (1999) attributed a *triangularis* Zone age to this strata. Mahmudy Gharaie *et al.* (2004) followed the age of Yazdi (1999), but this age is questionable.

GHALE-KALAGHU

Eight species and two biozones are assigned to this section (Table 4).

Table 3

Distribution chart of conodonts in the Howz-e-Dorah section, south of Tabas

Zones	Early to Late *rhenana*					Early to Late *crepida*			
Samples	Da	D1	D2	D3	D4	D6	HD1	D7	HD2
Ancyrodella curvata	–	1	1		1	–	–	–	–
Ancyrognathus asymmetricus	–	1	–		–	–	–	–	–
Icriodus al. alternatus	1	6	3	3	–	1	9	2	14
Palmatolepis sp. aff. *Pal. perlobata*	–	–	–		–	–	2	–	1
Pal. wolskajae	–	–	–		–	–	2	–	–
Polygnathus aequalis	1	9	2	7	–	–	–	–	–
P. brevilaminus	–	–	–		–	–	17	–	13
P. buzmakovi	–	–	–		–	–	2	–	2
P. evidens	–	3	1	1	2	–	–	–	–
P. politus	–	–	–		2	–	–	–	–
P. procerus	1	–	–		–	–	–	–	–
P. webbi	1	–	1		1	–	–	–	–
P. tabasianus n. sp.	–	–	–		–	–	4	–	2
Unassigned elements	–	1	6	5	8	–	4	–	12
Total	4	20	14	16	14	1	40	2	44
Biofacies	–	P-I	P-I	P-I	P	–	P-I	–	P-I

Explanations as in Table 1

Early to Late *rhenana* zones. *I. alternatus alternatus* and *P. politus* co-occur in this zone. Large placoderm remains have been placed in this interval.

Early to Late *crepida* zones. *I. alternatus alternatus*, *Pal.* sp. aff. *Pal. perlobata* and *Pal. wolskajae* were obtained from this biozone. Among other species is *P. tabasianus* n. sp.

Table 4

Distribution chart of conodont species in the Ghale Kalaghu section

Zones	E. to L. *rhenana*		E. to L. *crepida*		E. to L. *rhenana*	
Samples	GK1	GK2	GK6	GK7	Lb1	Lb3
Icriodus al. alternatus	1	2	61	2	2	3
Palmatolepis sp. aff. *Pal. perlobata*	–	–	5	–	–	–
Pal. wolskajae	–	–	3	–	–	–
Polygnathus communis group	–	–	2	–	–	–
P. brevilaminus	–	–	76	–	–	–
P. buzmakovi	–	–	10	–	–	–
P. politus	1	1	–	–	1	2
P. tabasianus n. sp.	–	–	10	–	–	–
Unassigned elements	–	–	121	–	–	–
Total	2	3	288	2	3	5
Biofacies	–	–	P-I	–	–	–

Samples from reworked blocks are shown as Lb1 and Lb3; explanations as in Table 1

BIOFACIES

The present inferences on palaeoecology and palaeoenvironment are based on field observations as well as on palaeontological and statistical data. Quantitative analyses of conodont biofacies are based on the concepts of Pohler and Barnes (1990); the biofacies were then compared with previous models (Sandberg and Dreseen, 1984; Sandberg *et al*., 1988) based primarily on sequences in North America and Europe. The abundance of *Icriodus* coupled with the absence of *Palmatolepis*, *Ancyrognathus* and *Ancyrodella* is typical of most Central Iranian conodont faunas such as the Chahriseh sequence which is characterized by icriodid-polygnathid and polygnathid-icriodid biofacies (Table 1). The number of *Polygnathus* elements decreases dramatically in the Early *triangularis* Zone with icriodid elements in greater abundance than polygnathids. Rhythmic changes between polygnathid-icriodid and icriodid-polygnathid associations occur throughout the *triangularis* Zone. The *triangularis* Zone biofacies in the Chahriseh section possibly resembles the inner shelf environment of the White Horse Pass succession in the Early *triangularis* Zone (Sandberg *et al*., 1988) though the biofacies of the late Frasnian in the Chahriseh section is less comparable to this.

The lowest samples from the Kal-e-Sardar section with a coral-rich bed show a polygnathid-icriodid biofacies, but in the middle part of this succession the *Polygnathus* elements represent more than 80% of the conodont faunas (samples K5H, K5J). This situation is similar to that of the end of *linguiformis* Zone at White Horse Pass, Nevada (Sandberg *et al*., 1988).

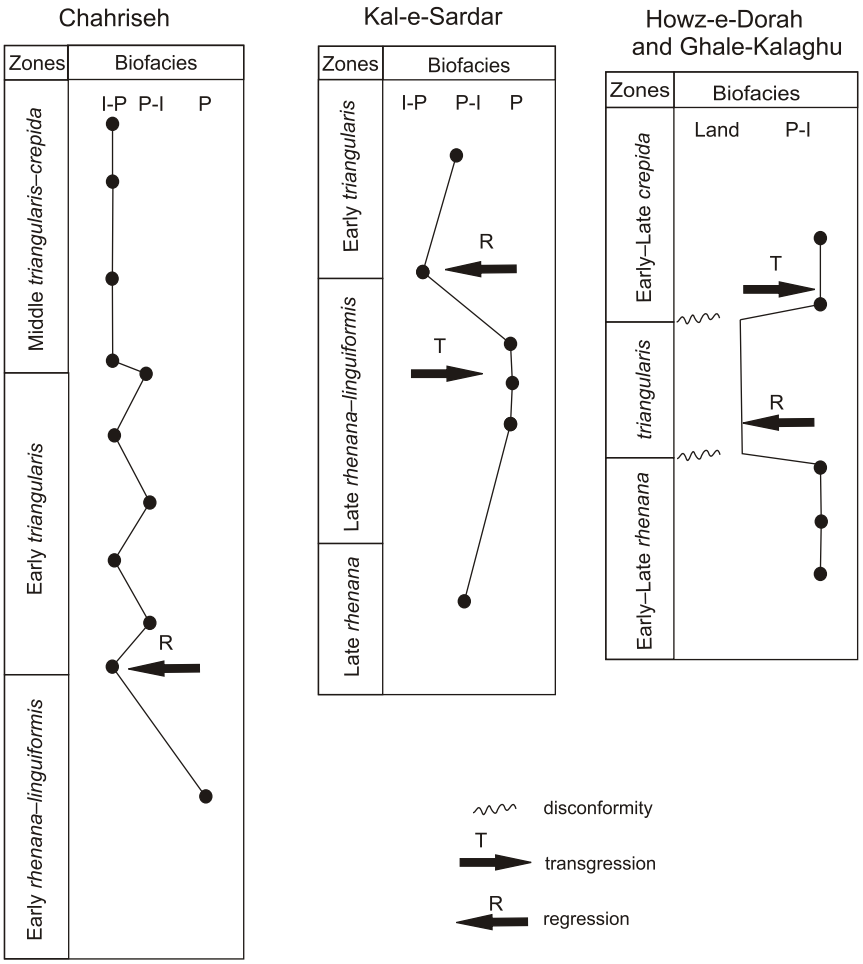

Fig. 8. Sea level changes pattern in the studied sections based on conodont biofacies against biozones

Explanations as in Table 1

Moreover, some species such as *P. procerus* and *P. politus* are predominant in these samples, indicating a favourable environment for these species. Coral beds at the base of the Kal-e-Sardar and in the middle part of the Chahriseh section (below the F–F boundary) accord with environments suggested for beds near the F–F boundary (Figs. 5 and 6). Biofacies in the upper part of the Kal-e-Sardar succession are very different to those in the middle of the succession. Conodonts from the lowest Famennian bed (sample Cly1, Early *triangularis* Zone), represent an icriodid-polygnathid biofacies. This accords with the shallowing environment from the late Frasnian into the early Famennian (Fig. 8).

In the Howz-e-Dorah and Ghale-Kalaghu sections, polygnathid-icriodid biofacies predominated during the *rhenana* and *crepida* zones. As mentioned before, the early Famennian terrigenous succession is inferred to have been deposited in a non-marine environment. These data and the lateral facies differences between the Shishtu Formation sections in Kal-e-Sardar, Howz-e-Dorah and Ghale Kalaghu accord with the southern Shotori Range being exposed during the regression in the early Famennian (*triangularis* Zone; Fig. 8).

REMARKS ON THE CAUSES OF THE F–F MASS EXTINCTION

Many causes have been proposed for the Late Devonian (F–F) mass extinction. Several authors, pointing to the presence of heavy metals (such as Ir and Ni) and assumed meteorite traces (such as melt breccia, microspherules and shocked minerals) at the extinction level, suggested extraterrestrial impact as the main cause of this mass extinction (McGhee, 1996, 2001; Reimold *et al*., 2005). However, Sandberg *et al*. (2002) preferred stepwise deterioration during the Frasnian with a series of impacts, sea level changes and a final crisis at the end of Frasnian. Others (Nicoll and Playford, 1993, and especially Girard *et al*., 1997) rejected the isotopic evidence for an impact scenario. Buggisch (1991) and Becker and House (1997) proposed a transgression-regression (T/R) scenario involving oxygen depletion, coupled with drastic sea level and climate changes. Bratton *et al*. (1999) preferred an oceanic anoxic event at the end of the Frasnian.

Racki (2005), on the basis of reports of magmatic activity in Siberia, eastern Europe and mid-Asia (e.g. Kiselev *et al*., 2004;

Pervov *et al*., 2005), discussed the strengths and weaknesses of the various theories, leaning towards volcanic/hydrothermal activity during the Upper Kellwasser Event as a possible explanation. A similar explanation was put forward by Hao *et al.* (2003) who invoked submarine rifting and hydothermal activity as the prime cause, pointing to enrichment of metals including nickel in deposits near the F–F boundary in the NW of China.

New research by Chow *et al*. (2005) and Averbuch *et al*. (2005), suggested that tectonic activity, weathering and organic carbon burial played a significant role in the extinction event. Hallam and Wignall (1999) stated there had been a sea level rise, but Yazdi (2000) argued for a sea level fall. The succession of the icriodid-polygnathid biofacies and the presence of reworked boulders in the early Famennian (Early to Late *triangularis* zones) succession supports the sea level fall scenario. Yazdi's (2000) view is therefore felt to be more consistent with presently available data, if eustatic regression was indead a primary cause of the large scale global extinction event.

Mahmudy Gharaie *et al*. (2003), on the basis of ^{13}C and REE anomalies in beds near to F–F boundary in Central Iran, suggested two possible causes: climate change and volcanic activity. Both are speculative as no account of biostratigraphic research was taken, especially of those studied based on conodonts. Subsequently Mahmudy Gharaie *et al*. (2004), suggested from iron-rich and clay minerals and isotopes (notably $^{87}Sr/^{86}Sr$) that very warm humid environments (greenhouse conditions) produced by a high concentration of CO_2 in the atmosphere caused the mass extinction. Such a warm and humid climate was said to result in deep weathering and subsequent increasing sedimentary transport from the continents, while volcanic activity was thought to be responsible for CO_2 increase in the atmosphere. Their work was mainly based on the presence of volcanic rocks and black shales in the Late Devonian successions of Iran. Evidence of synsedimentary volcanic activity can be seen in some sections of Central and Northern Iran (e.g. Geirud and Ardekan areas in Hairapetian and Yazdi, 2003; Wendt *et al*., 2005). However, contrary to the opinion of Mahmudy Gharaie *et al*. (2004), there is no high resolution palaeontological evidence of Frasnian volcanic events in Iran. To the contrary, the volcanic horizons of the Geirud Formation in the central Alborz Range can be attributed to the Famennian (Gaetani, 1965). Famennian ammonoids from a bed between two basaltic levels in the Geirud Formation were discovered by Dashtban (1995). Revision of the Dashtban material by Becker *et al*. (2004) confirmed a mid-late Famennian age and made possible correlation with contemporaneous ammonoid-bearing beds in the Shishtu Formation, representing the mid Famennian *Annulata* event. According to Hairapetian and Yazdi (2003, fig. 3), volcanic units in Dalmeh (the Ardekan area) formed in the early to mid Famennian (*triangularis* to *postera* zones). Therefore, these dated volcanic events in Alborz and Central Iran cannot be older than the early Famennian and therefore, this volcanic activity as the possible cause of late Frasnian mass extinction appears unsubstantiated.

Black shales from the Hutk and Gazestan localities, analysed by Mahmudy Gharaie *et al*. (2004) with regard to the F–F crisis, are also problematic. No precise age has been provided for black shales of the Gazestan section, whereas recent studies in the Hutk section revealed early Famennian conodont faunas (Gholamalian, 2006).

Dastanpour and Aftabi (2002) noted a decrease in ^{13}C and ^{18}O across the F–F boundary in Central Iran, regarding this as being due to either a meteoric impact or decay of organic matter.

Higher resolution biostratigraphic and geochemical data are thus needed from a larger number of sequences, not only in Iran but globally, in order that the controls on the global events across the F–F boundary can be effectively determined. But, consideration of the conodont biofacies and of field data indicates that a sea level fall is strongly associated with the Upper Kellwasser Event in Iran. Disconformity surfaces show the effect of tectonic events in the late Frasnian and early Famennian, as observed in sections such as at Howz-e-Dorah and Ghale-Kalaghu. The F–F boundary is associated with changes in conodont biofacies in the Chahriseh and Kal-e-Sardar successions. A combination of orogenic/epeirogenic movements and increased weathering may be a possible explanation for the late Frasnian crisis (in accordance with the opinion of Averbuch *et al*., 2005). Well-rounded redeposited blocks and deeply weathered sandstones in the southern Shotori Range successions (e.g. Mahmudy Gharaie *et al*., 2004) strengthen this opinion. Displacement of such blocks requires high energy flow, such as tsunami (e.g. Sandberg *et al*., 1988) or a powerful flood. These phenomena are less pronounced in the Kal-e-Sardar section (northern Shotori Range) than in the south and there is no sign of nonmarine conditions, though some black shale beds (8.7 m) are intercalated between beds K5J and Cly 1 (Fig. 6) and indicate deposition of carbon-rich siliciclastics in a marine environment possibly due to enhanced weathering on land. However, the environment became shallower at the top of this section (Kal-e-Sardar) and this trend continued into the Early *triangularis* Zone. The presence of major faults (such as the Naiband Fault) may be mainly responsible for this phenomenon by forming active horst-graben systems.

SYSTEMATIC PALAEONTOLOGY

Phylum **Conodonta** Pander, 1856
Order **Ozarkodinida** Dzik, 1976
Family Spathognathodontidae Hass, 1959
Genus *Ancyrodella* Ulrich and Bassler, 1926
Ancyrodella buckeyensis Ulrich and Bassler, 1926
Ancyrodella curvata (Branson and Mehl, 1934*a*)
(Fig. 9C)

D i a g n o s i s. — See Klapper (1989) and Ziegler and Sandberg (1990).

R a n g e. — Early *hassi* to end of *linguiformis* zones (Ji and Ziegler 1993, p. 52).

Ancyrodella buckeyensis Stauffer, 1938
(Fig. 9D)

D e s c r i p t i o n. — See Over (1997).

R a n g e. — According to Over (1997, figs. 7 and 8), this species has range of zones 12–13 of Klapper (1989).

Family Polygnathidae Bassler, 1925
Genus *Ancyrognathus* Branson and Mehl, 1934*a*
Ancyrognathus irregularis Branson and Mehl, 1934*a*
Ancyrognathus asymmetricus (Ulrich and Bassler, 1926)
(Fig. 9B)

D i a g n o s i s. — See Klapper (1990).

R a n g e. — Upper part of Zone 12 to the end of Zone 13 (Klapper, 1989,1990, p. 999), equating with the Late *rhenana–linguiformis* zones (Klapper and Becker, 1999). Associated taxa in the Howz-e-Dorah section indicate correlation with the *rhenana* Zone (Table 3).

Ancyrognathus triangularis Youngquist, 1945
(Fig. 9A)

D i a g n o s i s. — See Klapper (1990).

R a n g e. — From Zone 11 to the lower part of Zone 13 of Klapper (1990, p. 999) which is equivalent to the *jamieae* to Late *rhenana* zones, but Morrow (2000, p. 30–32) has reported this taxa from the *hassi* Zone at Tempiute Mountain and from the *linguiformis* Zone at Granite Mountain (USA). Associated conodonts in the Kal-e-Sardar sequence indicate an age-range from Late *rhenana* to *linguiformis* zones.

Order **Prioniodontida** Dzik, 1976
Family Icriodontidae Müller and Müller, 1957
Genus *Icriodus* Branson and Mehl, 1938
Icriodus expansus Branson and Mehl, 1938
Icriodus alternatus alternatus Branson and Mehl, 1934*a*
(Fig. 9O)

D i a g n o s i s. — See Sandberg and Dreesen (1984).

R a n g e. — This subspecies appeared in the Early *rhenana* Zone (Ziegler and Sandberg, 2000, p. 340–341), extending through to the Late *crepida* Zone (Sandberg and Dreesen, 1984).

Icriodus alternatus helmsi Sandberg and Dreesen, 1984
(Fig. 9Q)

D i a g n o s i s. — See Sandberg and Dreesen (1984).

R a n g e. — Late *rhenana* Zone to the end of the Middle *crepida* Zone (Ji and Ziegler, 1993, p. 55).

Icriodus alternatus mawsonae Yazdi, 1999
(Fig. 9R)

D i a g n o s i s. — See Yazdi (1999).

R a n g e. — The subspecies, discovered by Yazdi (1999) in beds assigned to the *crepida* Zone, has now been found with late Frasnian Late *rhenana* to *crepida* Zone conodonts in Kal-e-Sardar samples N, K5H and K5 (Table 2).

Icriodus aff. *I. cornutus* Sannemann, 1955*a*
(Fig. 10C, D)

D e s c r i p t i o n. — A form of *Icriodus* with a medial row of denticles as high as the lateral denticles and a large cusp at the posterior end of the platform connected to the medial row. The I element is unarched in side view but is down-curved beneath the large cusp.

R a n g e. — *I. cornutus* is reported to extend from the Middle *triangularis* zone to the Late *trachytera* Zone (Sandberg and Dreesen, 1984, p. 163), but considering its stratigraphic position and associated fauna, *I.* aff. *I. cornutus* seems to have appeared in the Early *triangularis* Zone.

Icriodus iowaensis iowaensis Youngquist and Peterson, 1947
(Fig. 9P, S–V)

D i a g n o s i s. — See Ji and Ziegler (1993).

R a n g e. — Early *hassi* to *jamieae* zones for first appearance (Gholamalian, 2006), and Early *rhomboidea* Zone (?) for extinction (Ji and Ziegler, 1993).

Icriodus multicostatus multicostatus Ji and Ziegler, 1993
(Fig. 10A)

D i a g n o s i s. — See Ji and Ziegler (1993).

R a n g e. — Middle *triangularis* Zone to Late *crepida* Zone (Ji and Ziegler, 1993, p. 57).

Icriodus xenium Nazarova, 1997
(Fig. 10B)

D e s c r i p t i o n. — A species of *Icriodus* characterized by an expanded platform with an acute anterior end (posterior end rounded), lateral denticles three to five in number on each side, triangular in transverse section; medial denticles small, rounded, smaller than and alternating with lateral ones. Posterior cusp extended backward.

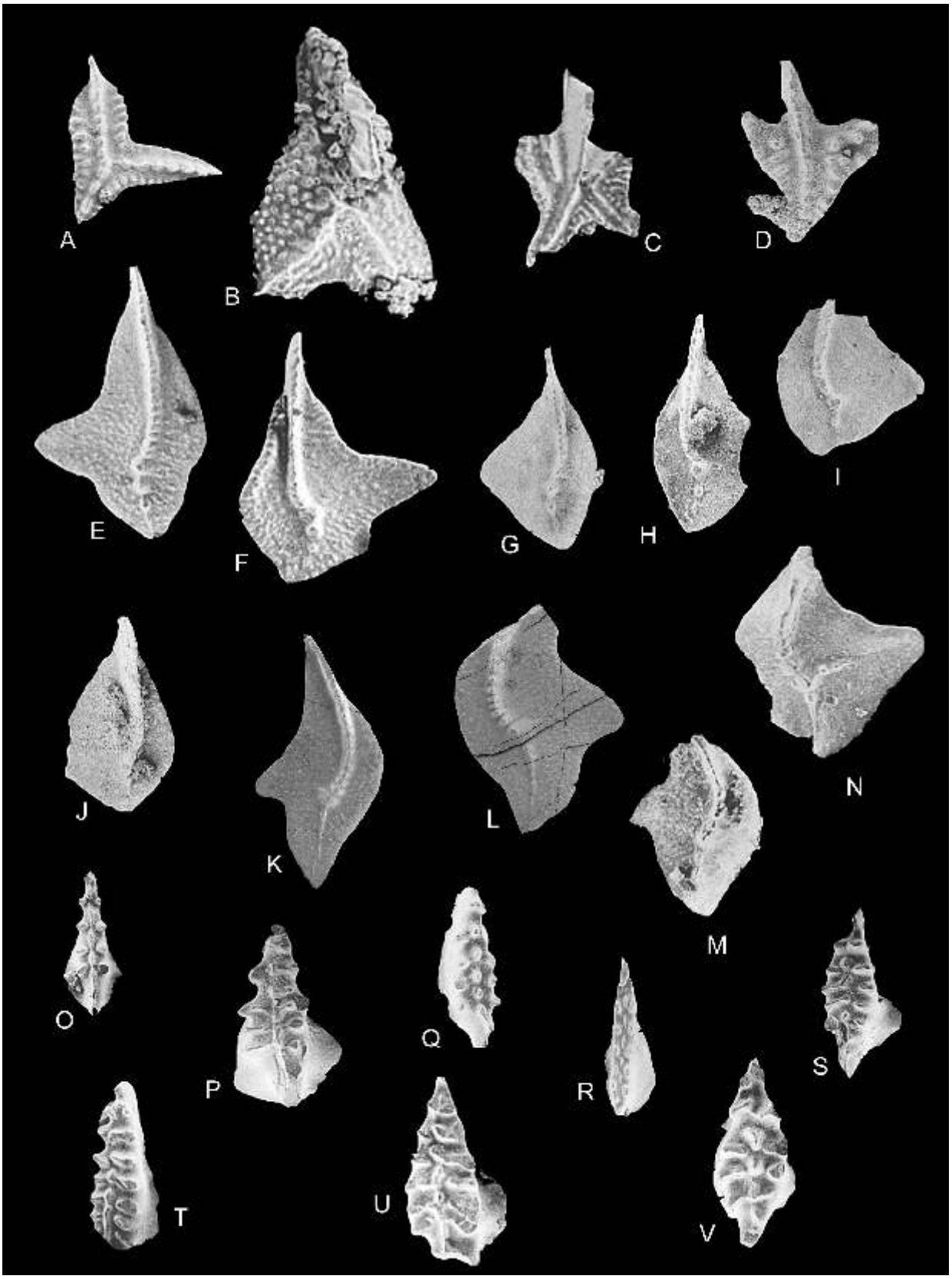
A
B
C
D
E
F
G
H
I
J
K
L
M
N
O
P
Q
R
S
T
U
V

R a n g e. — Mid Givetian to mid Frasnian *varcus–Ag. triangularis* zones (Nazarova, 1997, p. 639–640), but its range extends to late Frasnian (Late *rhenana–linguiformis* zones) in Kal-e-Sardar section and into the early Famennian (Early *triangularis* Zone) in the Chahriseh section.

Genus *Pelekysgnathus* Thomas, 1949
Pelekysgnathus inclinatus Thomas, 1949
Pelekysgnathus serradentatus Capkinoglu, 1991
(Fig. 10E, F)

C o m m e n t. — See Capkinoglu and Gedik (2000, p.77–78) for diagnostic features.

R a n g e. — According to Capkinoglu and Gedik (2000, table 4) from *triangularis* Zone to *crepida* Zone.

Order **Ozarkodinida** Dzik, 1976
Family Polygnathidae Bassler, 1925
Genus *Palmatolepis* Ulrich and Bassler, 1926
Palmatolepis perlobata Ulrich and Bassler, 1926
Palmatolepis gigas gigas Miller and Younquist, 1947
(Fig. 9F)

D i a g n o s i s. — See Ziegler and Sandberg (1990).

R a n g e. — Early *rhenana* Zone to the end of *linguiformis* Zone (Ziegler and Sandberg, 1990).

Palmatolepis aff. *Pal. perlobata* Ulrich and Bassler, 1926
(Fig. 9K, L)

D i a g n o s i s. — See Schülke (1995, p. 43) for *Palmatolepis perlobata.*

C o m m e n t s. — Because of breakage, many elements cannot be unequivocally identified as *Pal. perlobata*.

R a n g e. — Early *triangularis* Zone of the Kal-e-Sardar section.

Palmatolepis winchelli (Stauffer, 1938)
(Fig. 9E)

D i a g n o s i s. — See Klapper and Foster (1993).

R a n g e. — According to Klapper and Foster (1993, p. 31), this species occurs in zones 12 and 13 of Klapper (1989), equating with the Late *rhenana* to *linguiformis* zones.

Palmatolepis wolskajae Ovnatanova, 1969
(Fig. 9N)

D i a g n o s i s. —See Ziegler (1977).

R a n g e. — Early to Late *crepida* zones (Barskov *et al*., 1987; Ziegler and Sandberg, 1990, p.23–24).

Palmatolepis sp. aff. *Pal. perlobata* Ulrich and Bassler, 1926
(Fig. 9M)

R a n g e. — Early to Late *crepida* zones in the Howz-e-Dorah section.

Palmatolepis sp. A
(Fig. 9I, J)

R a n g e. — Late *rhenana* to *linguiformis* zones in the Kal-e-Sardar section.

Palmatolepis sp. B
(Fig. 9G, H)

R a n g e. — Late *rhenana* to *linguiformis* zones in the Kal-e-Sardar section.

Fig. 9. Conodonts from Howz-e-Dorah, Kal-e-Sardar, Ghale-Kalaghu and Chahriseh sections

A — *Ancyrognathus triangularis* Youngquist, 1945, upper view of EUIC 82101, sample K5, Kal-e-Sardar; **B** — *Ancyrognathus asymmetricus* (Ulrich and Bassler, 1926), upper view of EUIC 83103, sample D1, Howz-e-Dorah; **C** — *Ancyrodella curvata* (Branson and Mehl, 1934*a*), upper view of EUIC 82104, sample D2, Howz-e-Dorah; **D** — *Ancyrodella buckeyensis* Stauffer, 1938, upper view of EUIC 82106, sample K5H, Kal-e-Sardar; **E** — *Palmatolepis winchelli* (Stauffer, 1938), upper view of EUIC 82108, sample K5H, Kal-e-Sardar; **F** — *Palmatolepis gigas gigas* Miller and Younquist, 1947, upper view of EUIC 82109, sample K5, Kal-e-Sardar; **G**, **H** — *Plamatolepis* sp. B: **G** — upper view of EUIC 82110, sample K5H, Kal-e-Sardar, **H** — upper view of EUIC 82111, sample K5I, Kal-e-Sardar; **I**, **J** — *Palmatolepis* sp. A: **I** — upper view of EUIC 82112, sample K5H, Kal-e-Sardar, **J** — upper view of EUIC 82113, sample K5H, Kal-e-Sardar; **K**, **L** — *Palmatolepis* aff. *Pal. perlobata* Ulrich and Bassler, 1926: **K** — upper view of EUIC 82177, sample Cly 1, Kal-e-Sardar, **L** — upper view of EUIC 82178, sample Cly 1, Kal-e-Sardar; **M** — *Palmatolepis* sp. aff. *Pal. perlobata* Ulrich and Bassler, 1926, upper view of EUIC 82114, sample HD1, Howz-e-Dorah; **N** — *Palmatolepis wolskajae* Ovnatanova, 1969, upper view of EUIC 82115, sample GK6, Ghale-Kalaghu; **O** — *Icriodus altrenatus alternatus* Branson and Mehl, 1934*a*, upper view of EUIC 82116, sample K5, Kal-e-Sardar; **P**, **S**–**V** — *Icriodus iowaensis iowaensis* Youngquist and Peterson, 1947: **P** — upper view of EUIC 82118, sample K, Chahriseh, **S** — oblique upper view of EUIC 82123, sample M, Chahriseh, **T** — upper view of EUIC 82124, sample M, Chahriseh, **U** — upper view of EUIC 82125, sample M, Chahriseh, **V** — upper view of EUIC 82126, sample Y, Chahriseh; **Q** — *Icriodus alternatus helmsi* Sandberg and Dreesen, 1984, upper view of EUIC 82119, sample K5H, Kal-e-Sardar; **R** — *Icriodus alternatus mawsonae* Yazdi, 1999, upper view of EUIC 82120, sample K5, Kal-e-Sardar; all specimens are × 32


A
B
C
D
E
F
G
H
I
J
K
L
M
N
O
P
R
S
T
U
V

Genus *Polygnathus* Hinde, 1879
Polygnathus dubius Hinde, 1879
Polygnathus aequalis Klapper and Lane, 1985
(Fig. 10G, H)

D i a g n o s i s. — See Klapper and Lane (1985).

R a n g e. — In the Kal-e-Sardar section this is associated with conodonts indicative of the Late *rhenana* to *linguiformis* zones (Table 2), though it was formerly (Ji and Ziegler 1993, p. 74) reported as ranging from the *transitans* to the Early *rhenana* zones. An extension of range is thus indicated.

Polygnathus brevilaminus Branson and Mehl, 1934*a*
(Fig. 10J, K)

D i a g n o s i s. — See Schülke (1999).

R a n g e. — Late Frasnian and Famennian (Ji and Ziegler, 1993).

Polygnathus buzmakovi Kuzmin, 1990
(Fig. 11O, P)

D i a g n o s i s. — This is a species of *Polygnathus* with a narrow lanceolate asymmetrical platform that becomes shallower posteriorly. The carina is nodose, extending to a sharp posterior end. Ornament pf nodes or very short transverse ridges cover the platform.

R a n g e. — According to and Kuzmin (1990, p. 70) and Barskov *et al*. (1991, p. 15), this species occurs in the *crepida* Zone.

Polygnathus communis group Branson and Mehl, 1934*a*
(Fig. 12C–J)

C o m m e n t. — The *P. commuis* group includes many subspecies all characterized by the presence of a depression showing a thin keel immediately behind the small pit. Most authors refer to a small platform without ornament, but Barskov *et al*. (1991), Khalymbadzha *et al*. (1991) and Vorontsova (1993, 1996) accepted a broader interpretation for the *P. communis* group including forms with surface ornamentation. Barskov *et al*. (1991) and Vorontsova (1993, 1996) proposed a new genus, *Neopolygnathus*, for this group. All previous workers regarded the group as having originated in the Early *crepida* Zone. However, specifically the presence of specimens of this group in the *rhenana* to *linguiformis* zones in the Chahriseh succession, makes it necessary to re-consider the early evolution of the *P. communis* group. Conodont assemblages from near the Frasnian–Famennian boundary in the Chahriseh sequence demonstrate a preference of the group for the icriodid-polygnathid and the polygnathid-icriodid biofacies, both interpreted as shallow water environments (Fig. 8).

Previous workers e.g. Ji and Ziegler (1993) reported the *P. communis* group from deeper environments in the Famennian with *Palmatolepis*, but close association with near-shore environments in the late Frasnian and early Famennian (*rhenana* to *triangularis* zones) seems evident from data presented here. Ovnatanova and Kononova (2001, pl. 23, figs. 15–24) figured several specimens identified as *Polyganthus aspelundi*, but two of their figures (17 and 18) have a depression behind the basal pit and belong, in fact, to *P. communis*. From these new data, I conclude that the *P. communis* group appeared in the late Frasnian. This group has also been recognized in Frasnian samples from the Kerman area of SE Iran (Gholamalian, 2006), the elements being very similar to those from Chahriseh.

R a n g e. — *rhenana–linguiformis* zones interval (the present paper) to the late Tournaisian *anchoralis-latus* Zone (Ji and Ziegler, 1993, p. 48).

Polygnathus evidens Klapper and Lane, 1985
(Fig. 10M, N)

D i a g n o s i s. — See Klapper and Lane (1985).

R a n g e. — Early to Late *rhenana* zones (Ovnatanova and Kononova, 2001).

Polygnathus politus Ovnatanova, 1969
(Fig. 10R–V)

Fig. 10. Conodonts from Howz-e-Dorah, Kal-e-Sardar and Chahriseh sections

A — *Icriodus multicostatus multicostatus* Ji and Ziegler, 1993, upper view of EUIC 82128, sample EX6, Chahriseh; **B** — *Icriodus xenium* Nazarova, 1997, upper view of EUIC 82130, sample K5, Kal-e-Sardar; **C**, **D** — *Icriodus* aff. *I. cornutus* Sannemann, 1955*a*: **C** — upper view of EUIC 82134, sample T4, Chahriseh, **D** — upper view of EUIC 82135, sample T4, Chahriseh; **E**, **F**— *Pelekysgnathus serradentatus* Capkinoglu, 1991: **E** — upper view of EUIC 82132, sample F-F1, Chahriseh, **F** — lateral view of EUIC 82133, sample F-F7, Chahriseh; **G**, **H** — *Polygnathus aequalis* Klapper and Lane, 1985: **G** — upper view of EUIC 82136, sample D1, Howz-e-Dorah, **H** — upper view of EUIC 82137, sample K5H, Kal-e-Sardar; **I** — *Polygnathus* sp. A, upper view of EUIC 82138, sample T3A, Chahriseh; **J**, **K** — *Polygnathus brevilaminus* Branson and Mehl, 1934*a*: **J** — upper view of EUIC 82150, sample F-F7, Chahriseh, **K** — upper view of EUIC 82151, sample T3A, Chahriseh; **L** — *Polygnathus* sp. B, upper view of EUIC 82140, sample T4, Chahriseh; **M**, **N** — *Polygnathus evidens* Klapper and Lane, 1985: **M** — oblique upper view of EUIC 82141, sample K5, Kal-e-Sardar, **N** — upper view of EUIC 82143, sample EX1, Chahriseh; **O**, **P**— *Polygnathus procerus* Sannemann, 1955*b*: **O** — upper view of EUIC 82145, sample K5H, Kal-e-Sardar, **P** — upper view of EUIC 82146, sample K5, Kal-e-Sardar; **R**–**V** — *Polygnathus politus* Ovnatanova, 1969: **R**, **S** — upper and lateral view of EUIC 82147, sample K5, Kal-e-Sardar, **T** — lower view of EUIC 82148, sample K5, Kal-e-Sardar, **U**, **V** — upper and lower view of EUIC 82179, sample EX1, Chahriseh; all specimens are × 32

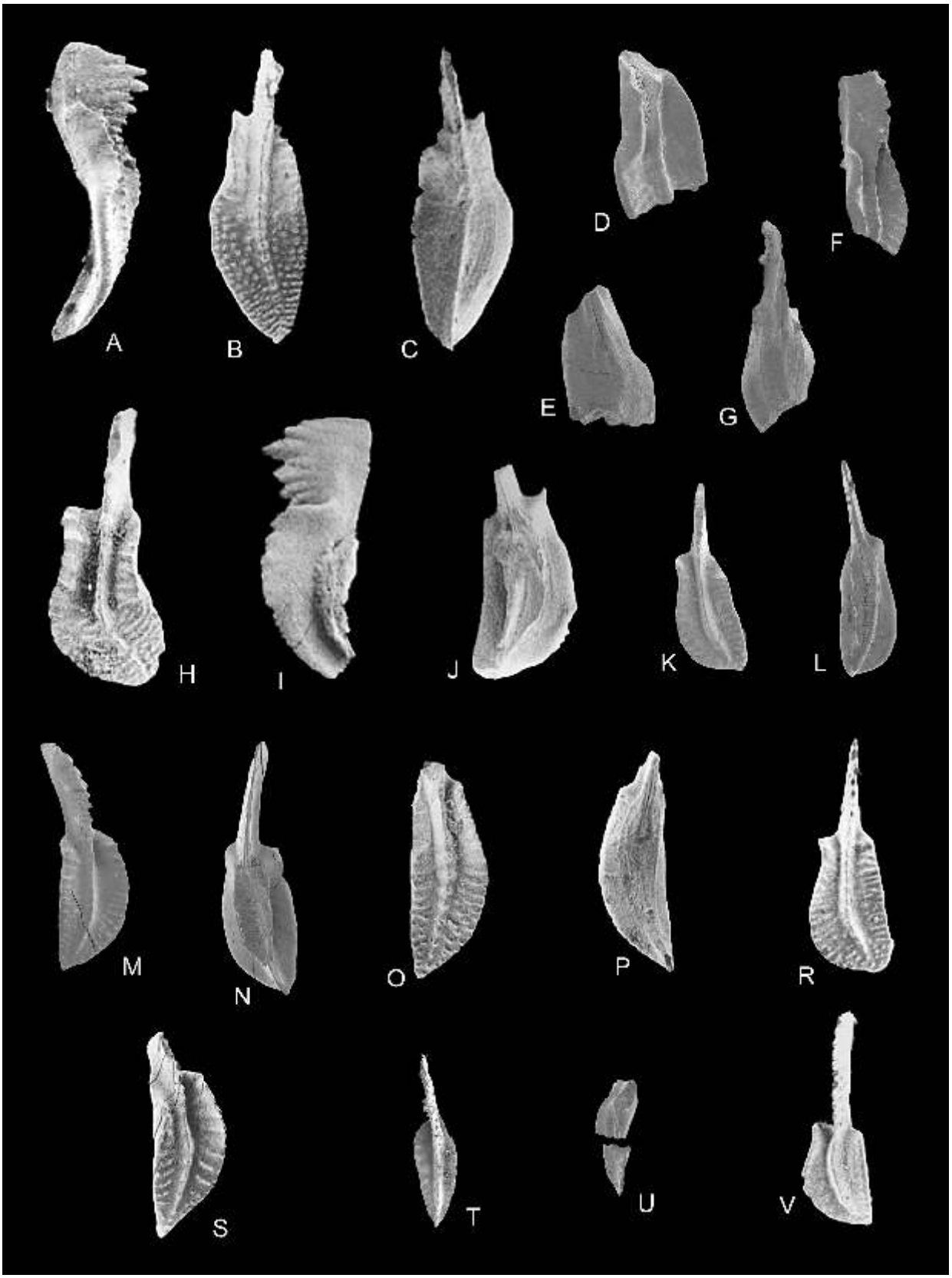
A
B
C
D
E
F
G
H
I
J
K
L
M
N
O
P
R
S
T
U
V

D i a g n o s i s. — See Ovnatanova and Kononova (2001).

R a n g e. — Lower to Uppermost *gigas* zones (Ovnatanova and Kononova, 1996, 2001), equating with the Early *rhenana* to *linguiformis* zones of current nomenclature.

Polygnathus procerus Sannemann, 1955*b*
(Fig. 10O, P)

D i a g n o s i s. — See Schülke (1999).

R a n g e. — Middle *falsiovalis* Zone into Late *crepida* Zone. (Ji and Ziegler, 1993).

Polygnathus tabasianus n. sp.
(Fig. 11A–G)

H o l o t y p e. — EUIC 82155 sample HD1, Howz-e-Dorah section, Figure 11A–C.

P a r a t y p e. — EUIC 82181 sample HD1, Howz-e-Dorah section, Figure 11F, G.

E t y m o l o g y. — Tabas, a small town in East-Central Iran near the Kal-e-Sardar, Howz-e-Dorah and Ghale-Kalaghu sections.

M a t e r i a l. — Four Pa elements from sample HD1, two from HD2, Howz-e-Dorah, ten from sample GK6, Ghale-Kalaghu section.

D i a g n o s i s. — This species is discriminated from *P. ratebi* Yazdi (1999) by its shallower adcarinal troughs and having nodes instead of transverse ridges on the platform. It differs from *P. nodocostatus* by having nodes instead of nodose costae on the platform and a carina that does not extend to the posterior end. *P. buzmakovi* Kuzmin (1990) is similar, but the platform of *P. tabasianus* is wider, the free blade is shorter and the carina does not reach the posterior end of the platform.

D e s c r i p t i o n. — Pa elements with an asymmetric and nodose platform constricted anteriorly and with upturned platform margins, also anteriorly, making moderate anterior troughs shallowing towards mid-length. Platform broad at mid-length, with outer posterior platform strongly arched downward, bearing small nodes or short transverse ridges. Free blade is very short with four denticles, the second and third being higher than the others. The carina consists of discrete nodes extending for four-fifths of platform length, and does not reach the posterior end. Basal cavity small, located in the anterior third of the platform. Keel extends to the posterior end of platform.

R a n g e. — Early to Late *crepida* zones is suggested because of association with *I. alternatus alternatus*, the *P. communis* group, *P. buzmakovi* and *Pal. wolskajae* in the Howz-e-Dorah and Ghale-Kalaghu sections.

Polygnathus tenellus Ji and Ziegler, 1993
(Fig. 11T, U)

D i a g n o s i s. — See Ji and Ziegler (1993).

R a n g e. — Early *rhenana* to Early *triangularis* zones (Ji and Ziegler, 1993).

Polygnathus vachiki n. sp.
(Fig. 11H–L)

H o l o t y p e. — EUIC 82156 sample K5X Kal-e-Sardar section, Figure 11H, I.

P a r a t y p e. —EUIC 82182, sample K5, Kal-e-Sardar section, Figure 11K, L.

E t h y m o l o g y. — In honor of the young Iranian vertebrate palaeontologist, Vachik Hairapetian.

M a t e r i a l. — Two Pa elements from sample K5H, eight from K5, four from K5X, Kal-e-Sardar section.

D i a g n o s i s. — The species can be discriminated from *P. webbi* and *P. samueli* by more pronounced constriction of the platform anterior and a left anterior margin that is higher than the right.

D e s c r i p t i o n. — The new species is characterised by pronounced constriction of the anterior half of the platform to form a collar, a left anterior margin that is higher than the right and a platform surface that is ornamented by irregular transverse ridges and discrete small nodes. The platform widens posteriorly and is curved gently downwards. Adcarinal troughs are deep anteriorly but disappear in the mid-part of the platform. Outer and inner lobes are wide. Carina fused, not reaching the posterior end. Blade joins anterior of platform without any angle. The free blade is short and high with the third anterior denticle highest.

R a n g e. — Late *rhenana–linguiformis* zones according to associated species in the Kal-e-Sardar samples (Table 2).

Fig. 11. Conodonts from Howz-e-Dorah, Kal-e-Sardar and Chahriseh sections

A–**G** — *Polygnathus tabasianus* n. sp.: **A**–**C** — lateral, upper and lower view of EUIC 82155, holotype, sample HD1, Howz-e-Dorah, **D**, **E** — upper and lower view of EUIC 82180, sample HD1, Howz-e-Dorah, **F**, **G** — oblique upper and lower view of EUIC 82181, paratype, sample HD1, Howz-e-Dorah; **H**–**L** — *Polygnathus vachiki* n. sp.: **H**, **I** — upper and lateral view of EUIC 82156, holotype, sample K5X, Kal-e-Sardar, **J** — lower view of EUIC 82157, sample K5X, Kal-e-Sardar, **K**, **L** — upper and lower view of EUIC 82182, paratype, sample K5, Kal-e-Sardar; **O**, **P** — *Polygnathus buzmakovi* Kuzmin, 1990, upper and lower view of EUIC 82158, sample HD1, Howz-e-Dorah; **M**, **N**, **R**, **S** — *Polygnathus webbi* Stauffer, 1938: **M**, **N** — upper and lower view of EUIC 82183, sample K5, Kal-e-Sardar, **R** — upper view of EUIC 82161, sample K5H, Kal-e-Sardar, **S** — upper view of EUIC 82163, sample K5H, Kal-e-Sardar; **T**, **U** —— *Polygnathus tenellus* Ji and Ziegler, 1993, upper and lower view of EUIC 82184, sample Cly 1, Kal-e-Sardar; **V** — *Polygnathus* sp. C, upper view of EUIC 82164, sample K5, Kal-e-Sardar; all specimens are × 35

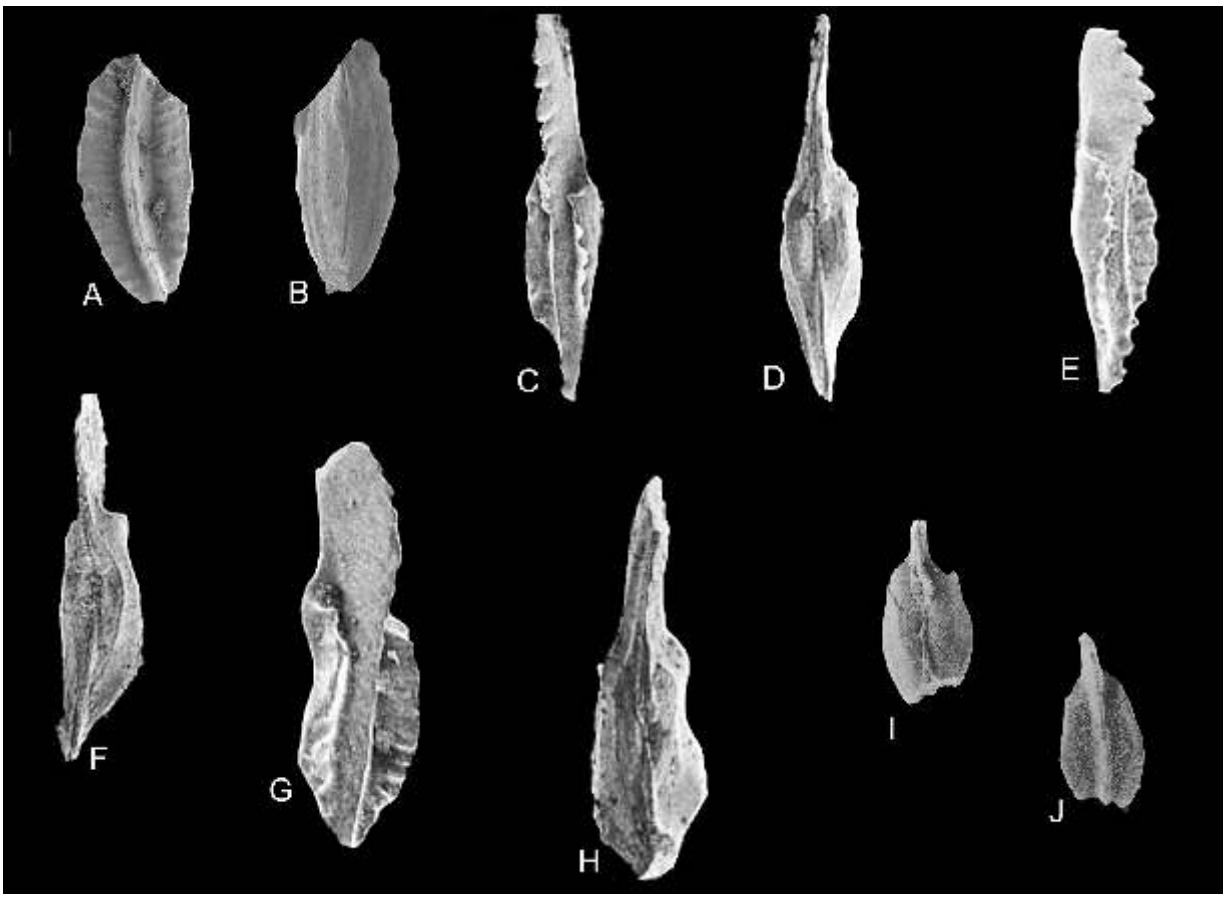

Fig. 12. Conodonts from Kal-e-Sardar and Chahriseh sections

A, **B** — *Polygnathus* cf. *P. webbi* Miller and Younquist, 1947, upper and lower view of EUIC 82185, sample Cly 1, Kal-e-Sardar; **C**–**J** — *Polygnathus communis* group Branson and Mehl, 1934*a*: **C**, **D** — upper and lower view of EUIC 82167, sample T3A; **E**, **F** — upper and lower view of EUIC 82169, sample Q; **G**, **H** — upper and lower view of EUIC 82173, sample F-F7; **I**, **J** — upper and lower view of EUIC 82186, sample F-F10; all figures **C**–**J** are from Chahriseh section; all specimens are × 50

Polygnathus webbi Stauffer, 1938
(Fig. 11M, N, R, S)

D i a g n o s i s. — See Ji and Ziegler (1993).

R a n g e. — Early *falsiovalis* to end of *linguiformis* Zone (Ji and Ziegler, 1993).

Polygnathus cf. *P. webbi* Stauffer, 1938
(Fig. 12A, B)

D i a g n o s i s. — See Ji and Ziegler (1993).

R a n g e. — Early *triangularis* Zone, Kal-e-Sardar section.

Polygnathus sp. A
(Fig. 10I)

D e s c r i p t i o n. — This species is characterised by an asymmetrical platform with expanded outer platform-half and weak transverse ridges. The anterior part of the platform is constricted, becoming wider near mid-length. The carina is fused, reaching to the posterior end and forming a tip. The basal cavity is small, located in the first third of the platform.

R a n g e. — Associated, at Chahriseh, with early Famennian (Early *triangularis* Zone) conodonts.

Polygnathus sp. B
(Fig. 10L)

D e s c r i p t i o n. — This species is characterised by its narrow, elongate, slightly asymmetrical platform with its anterior margins upturned: this part is narrow and constricted, but widens at platform mid-length. Adcarinal troughs are deep anteriorly, becoming shallower posteriorly. The outer platform margin is slightly expanded. The anterior two-thirds of the platform is smooth, the remainder being covered by short transverse ridges or nodes.

R a n g e. — Associated species in the Kal-e-Sardar and Chahriseh sections suggest an age-range of late Frasnian to early Famennian (Late *rhenana* to Early *triangularis* zones).

Polygnathus sp. C
(Fig. 11V)

C o m m e n t. —This species is recognized by its long blade and more or less smooth asymmetrical platform constricted anteriorly and its expanding outer platform-half. The blade is as long as the platform. The carina is smooth, reaching the posterior end.

R a n g e. — Late *rhenana* to *linguiformis* zones, Kal-e-Sardar.

CONCLUSION

Investigation into the Frasnian–Famennian boundary in Central Iran on the basis of conodont biostratigraphy and biofacies analysis has been conducted at four sections: Chahriseh (Esfahan), and Kal-e-Sardar, Howz-e-Dorah and Ghale-Kalaghu (Shotori Range). Two new conodont species are described; *Polygnathus vachiki* n. sp. from late Frasnian of Kal-e-Sardar and *P. tabasianus* n. sp. from the early Famennian of Howz-e-Dorah and Ghale-Kalaghu in the Shotori Range. On the basis of biostratigraphic data and associated faunas, new age ranges are proposed for *Polygnathus aequalis, Icriodus xenium* and *I. alternatus mawsonae*. Some initial forms of the *P. communis* group are reported from late Frasnian beds for the first time.

Conodont biofacies analysis in the beds close to the F–F boundary in Central Iran shows a considerable sea level fall, continued by marine shallowing or complete regression (e.g. southern Shotori Range). The presence of large blocks that are scattered in a deeply weathered sandstone matrix (in the southern Shotori Range) and in black shales (northern part), indicates considerable orogenic/epeirogenic activity around the Frasnian–Famennian boundary. The palaeotectonic activity in the western part of Central Iran appeared in form of epeirogenic and vertical movements and caused sea level fall (shallowing).

Acknowledgments. The research was facilitated by many friends. Profs J. A. Talent, G. Klapper and M. C. Perri provided useful literature not easily available in Iran; Prof. P. Bultynck and Dr. G. Racki made critical comments on the text and on the taxonomic identifications, Vachik Hairapetian provided much help in sampling and with technical comments; Drs Mohammad-Reza Kebriaei and Majid Mirzaei helped with fieldwork and acid leaching; Ms Davoodi and M. Dorushy (Azar Refractory Company of Esfahan) provided SEM micrographs; the Department of Geology, University of Hormozgan, provided financial and technical support; and my wife provided support at all stages.

REFERENCES

ASHOURI A. (1990) — Devonian and Carboniferous Conodont Faunas from Iran. Ph.D. Thesis, University of Hull.

AVERBUCH O., TRIBOVILLARD N., DEVLEESCHOUWER X., RIQUIER L., MISTIAEN B. and VAN VLIET-LANOE B. (2005) — Mountain building-enhanced continental weathering and organic carbon burial as major causes for climatic cooling at the Frasnian-Famennian boundary (c. 376 Ma)? Terra Nova, **17**: 25–34.

BARSKOV I. S., ALEKSEEV A. S., KONONOVA L. I. and MIGDISOVA A. V. (1987) — Atlas of Upper Devonian and Carboniferous conodonts. Izdat. Moskov. Univ. Geol. Fakul. Moscow.

BARSKOV I. S., VORONTSOVA T. N., KONONOVA L. I. and KUZMIN A. V. (1991) — Oprdelitel konodontov devona i nizhnego karbona. Izdat. Moskov. Univ. Geol. Fakul. Moscow.

BECKER R. T., ASHOURI A. R. and YAZDI M. (2004) — The upper Devonian *Annulata* event in the Shotori Range (eastern Iran). Neues Jahrb. Geol. Paläont. Abh., **231**: 119–143.

BECKER R. T., HOUSE M. R., KIRCHGASSER W. T. and PLAYFORD P. (1991) — Sedimentary and faunal changes across the Frasnian/Famennian boundary in the Canning Basin of Western Australia. Historical Biology, **5**: 183–196.

BECKER R. T. and HOUSE M. R. (1997) — Sea-level changes in the Upper Devonian of the Canning Basin, Western Australia. Courier Forsch.-Inst. Senckenberg, **199**: 129–146.

BRATTON J., BERRY W. B. N. and MORROW J. (1999) — Anoxia pre-dates Frasnian-Famennian boundary mass extinction horizon in the Great Basin, USA. Palaeogeogr. Palaeoclimat. Palaeoecol., **154**: 275–292.

BRICE D., MISTIAEN B. and ROHART J. C. (1999) — New data on distribution of brachiopods, rugose corals and stromatoporids in the Upper Devonian of central and eastern Iran, palaeobiogeographic implications. Ann. Soc. Géol. Nord, **7**: 21–32.

BRICE D. and KEBRIA-EE M. (2000) — A new species of Leiorhynchiidae rhynchonellid brachiopod from the Frasnian of Chahriseh, Esfahan Province, central Iran. Ann. Soc. Géol. Nord, **8**: 61–66.

BUGGISCH W. (1991) — The global Frasnian-Famennian Kellwasser Event. Geol. Rundsch., **80**: 49–72.

CAPKINOGLU S. (1991) — A new *Pelekysgnathus* species from the Lower Famennian of the Taurides, Turkey. Bollet. Soc. Paleont. Italiana, **30**: 349–353.

CAPKINOGLU S. and GEDIK I. (2000) — Late Devonian conodont fauna of the Gumusali Formation, the eastern Taurides, Turkey. Turkish J. Earth Sc., **9**: 69–89.

CHEN D. Z., QING H. R. and LI R. W. (2005) — The Late Devonian Frasnian-Famennian (F/F) biotic crisis: Insights from $\delta^{13}C_{carb}$, $\delta^{13}C_{org}$ and $^{87}Sr/^{86}Sr$ isotopic systematics. Earth Planet. Sc. Lett., **235**: 151–166.

CHOW N., GEORGE A. D. and TRINAJSTIC K. M. (2004) — Tectonic control on development of a Frasnian-Famennian (Late Devonian) palaeokarst surface, Canning Basin reef complexes, northwestern Australia. Australian J. Earth Sc., **51**: 911–917.

DASHTBAN H. (1995) — Upper Devonian Goniatites (Famennian) from central Alborz (in Persian with English abstract). Geosc. Sc. Quart. J., **14** (4): 36–43.

DASTANPOUR M. and AFTABI A. (2002) — The cause of biomass extinction at the Frasnian-Famennian boundary, the Kerman Province southeastern Central Iran. Islamic Republic of Iran J. Sc., **13**: 45–49.

GAETANI M. (1965) — The geology of the upper Djadjerud and Lar valleys (north Iran), II. Rivista Italiana Palaeont. Strat., **71** (3): 679–770.

GHAVIDEL-SYOOKI M. (2001) — Palynostratigraphy and paleogeography of the Late Devonian in northeastern Esfahan city, Central Iran. In: Proc. IX Internat. Palynol. Congress (eds. D. K.

Goodman and R. T. Clarke): 37–51. Am. Ass. Strat. Palynol. Texas. Houston.

GHOLAMALIAN H. (1998) — Biostratigraphy of Late Devonian sediments in Chahriseh area north-east of Esfahan based on conodont species. In: UNESCO-IGCP Project 421, North Gondwanan mid-Palaeozoic bioevent/biogeography patterns in relation to crustal dynamics, Esfahan meeting IGCP 421, December 5–20, 1998 (eds. R. Mawson, J. A. Talent and G. Wilson). Abstract book, **13**. Geol. Dep. Univ. Esfahan.

GHOLAMALIAN H. (1999) — Color alteration index and its application on Late Devonian conodonts in Kuh-e-Kaftari, NE of Esfahan. Geol. Soc. Iran, III Symp.: 438–440. Shiraz.

GHOLAMALIAN H. (2003) — Age implication of Late Devonian conodonts from the Chahriseh area northeast of Esfahan, central Iran. Courier Forsch.-Inst. Senckenberg, **245**: 201–207.

GHOLAMALIAN H. (2006) — Biostratigraphy of Late Devonian sequence in Hutk section (North of Kerman) based on conodonts (in Persian with English abstract). Geosc. Sc. Quart. J., **59** (15): 94–101.

GIRARD C., ROBIN E., ROCCHIA R., FROGET L. and FEIST R. (1997) — Search for impact remains at the Frasnian-Famennian boundary in the stratotype area, southern France. Palaeogeogr. Palaeoclimat. Palaeoecol., **132**: 391–397.

GOLONKA J., ROSS M. I. and SCOTESE C. R. (1994) — Phanerozoic palaeogeographic and palaeoclimatic modelling maps. In: Pangea: Global Environments and Resource (eds. A. F. Embry, B. Beauchamp and D. J. Glass). Canadian Soc. Petrol. Geol., Mem., **17**: 1–48.

HAIRAPETIAN V. and YAZDI M. (2003) — Late Devonian Conodonts from Dalmeh section, northeastern Ardekan, Central Iran. Courier Forsch.-Inst. Senckenberg, **245**: 209–225.

HALLAM A. and WIGNALL P. B. (1999) — Mass extinctions and sea level changes. Earth Sc. Rev., **48**: 217–250.

HAO W., JIANG D., YAO J., BAI S. and WANG X. (2003) — Frasnian-Famennian boundary events in Tarim Basin, Xinjiang, northwest China. Sc. China, Ser. D, **46** (9): 865–871

HASHEMI H. and PLAYFORD G. (1998) — Upper Devonian palynomorphs of the Shishtu Formation, Central Iran Basin, east-central Iran. Palaeontographica Abt. B, **246**: 115–212.

HOUSE M. R., BECKER R. T., FEIST R., GIRARD C. and KLAPPER G. (2000) — The Frasnian/Famennian boundary GSSP at Coumiac, southern France. Courier Forsch.-Inst. Senckenberg, **225**: 59–75.

JAFARIAN M. A. (2000) — Late Devonian index brachiopoda of north-east Esfahan in correlation with other regions. Islamic Rep. of Iran J. Sc., **11**: 221–231.

JI Q. and ZIEGLER W. (1993) — The Lali section. An excellent reference section for Upper Devonian in south China. Courier Forsch.-Inst. Senckenberg, **157**.

KHALYMBADZHA V. G., SHINKARYOV G. Y. and GATOVSKY Y. A. (1991) — Novyye famenskiye polygnatidy (konodonty) Yuzhnogo Kazakhstana. Paleont. Zhurnal, **1991** (2): 56–64.

KISELEV A. I., YARMOLYUK V. V., EGOROV K. N., MASLOVSKAYA M. N., CHEMYSHOV R. A. and KOVALENKO V. I. (2004) — Composition and source of Middle Palaeozoic basalts of Vilyui Palaeorift. Dokl. Earth Sc., **397**: 641–646.

KLAPPER G. (1989) —The Montagne Noire Frasnian (Upper Devonian) conodont succession. In: Proc. II Internat. Symp. Devonian System (eds. N. J. McMillan, A. F. Embry and D. G. Glass). Canadian Soc. Petrol. Geol., **3**: 449–468.

KLAPPER G. (1990) — Frasnian species of Late Devonian conodont genus *Ancyrognathus*. J. Palaeont., **64** (6): 998–1025.

KLAPPER G. and BECKER R. T. (1999) — Comparison of Frasnian (Upper Devonian) conodont Zonations. Bollet. Soc. Palaeont. Italiana, **37**: 339–348.

KLAPPER G., FEIST R., BECKER R. T. and HOUSE M. R. (1993) — Definition of the Frasnian/Famennian stage boundary. Episodes, **16**: 433–441.

KLAPPER G. and FOSTER C. T. (1993) — Shape analysis of Frasnian species of the Late Devonian conodont genus *Palmatolepis*. J. Palaeont., **67**, Suppl., 4, Mem., 32: 1–35.

KLAPPER G. and LANE H. R. (1985) — Upper Devonian (Frasnian) conodonts of the *Polygnathus* biofacies, N. W. T., Canada. J. Palaeont., **59**: 904–951.

KUZMIN A. V. (1990) — Asimmetricheskiye pary platformennykh elementov u nekotorykh predstaviteley roda *Polygnathus* (konodonty). Paleont. Zhurnal, **1990** (4): 66–74.

MAHMUDY GHARAIE M. H., MATSUMOTO R., KAKUWA Y. and MILROY P. G. (2003) — Geochemical evidence for environmental changes at Frasnian-Famennian boundary leading to the mass extinction. Geochim. Cosmochim. Acta, **67**: A268.

MAHMUDY GHARAIE M. H., MATSUMOTO R., KAKUWA Y. and MILROY P. G. (2004) — Late Devonian facies variety in Iran: volcanism as a possible trigger of the environmental perturbation near the Frasnian-Famennian boundary. Geol. Quart., **48** (4): 323–332.

McGHEE G. R. Jr. (1996) — The Late Devonian mass extinction, the Frasnian/Famennian crisis. In: Critical Moments in Palaeobiology and Earth History Series(eds. D. Bottjer and R. K. Bambach). Columbia Univ. Press. New York.

McGHEE G. R. Jr. (2001) — The multiple hypothesis for mass extinction: A comparison of Late Devonian and the Late Eocene. Palaeogeogr. Palaeoclimat. Palaeoecol., **176**: 47–58.

MISTIAEN B. and GHOLAMALIAN H. (2000) — Stromatoporoids and some tabulate corals from Chahriseh area (Esfahan Province, Central Iran). Ann. Soc. Géol. Nord, **8**: 81–91.

MISTIAEN B., GHOLAMALIAN H., GOURVENNEC R., PLUSQUELLC Y., BIGEY F., BRICE D., FEIST M., FEIST R., GHOBADI POUR M., KEBRIA-EE M., MILHAU B., NICOLLIN J. P., ROHART J. C., VACHARD D. and YAZDI M. (2000) — Preliminary data on the Upper Devonian (Frasnian, Famennian) and Permian fauna and flora from the Chahriseh area (Esfahan Province, Central Iran). Ann. Soc. Géol. Nord, **8**: 93–102.

MORROW J. (2000) — Shelf to basin lithofacies and conodont paleoecology across Frasnian/Famennian (F-F, mid-Late Devonian) boundary, central Geat Basin (western U.S.A.). Courier Forsch.-Inst. Senckenberg, **219**: 1–57.

NAZAROVA V. M. (1997) — New conodont species of the genus *Icriodus* from the Eifelian and Frasnian of the Russian Platform. Paleont. Zhurnal, **1997** (6): 636–640.

NICOLL R. S. and PLAYFORD P. E. (1993) — Upper Devonian anomalies, conodont zonation and the Frasnian-Famennian boundary in the Canning Basin, Western Australia. Palaeogeogr. Palaeoclimat. Palaeoecol., **104**: 105–113.

OVER J. D. (1997) — Conodont biostratigraphy of the Java Formation (Upper Devonian) and the Frasnian-Famennian boundary in western New York State. Geol. Soc. Am. Spec. Pap., **321**: 161–177.

OVNATANOVA N. (1969) — Novye verkhnedevonskie konodonty tsentral'nykh rayonov Russkoy Platformy in Timana. In: Fauna i Stratigraphiya Paleozoya Russkoya Platformy, 39–141. Nedra. Moscow.

OVNATANOVA N. S. and KONONOVA L. I. (1996) — New Frasnian polygnathids from central areas of the Russian Platform. Paleont. Zhurnal, **1996** (1): 52–60.

OVNATANOVA N. S. and KONONOVA L. I. (2001) — Conodonts and Upper Devonian (Frasnian) biostratigraphy of central regions of Russian platform. Courier Forsch.-Inst. Senckenberg, **233**.

PERVOV V. A., BOGOMOLOV E. S., LARCHENKO V. A., LEVSKII L. K., MINCHENKO G. V., SABLUKOV S. M., SERGEEV S. A. and STEPANOV V. P. (2005) — Rb-Sr age of kimberlites of Pionerskaya Pipe, Arkhangel'sk Diamondiferous Province. Dokl. Earth Sc., **400**: 67–71.

POHLER S. M. and BARNES C. R. (1990) — Conceptual models in conodont paleoecology. Courier Forsch.-Inst. Senckenberg, **118**: 409–440.

RACKI G. (2005) — Toward understanding Late Devonian global events: few answers, many questions. In: Understanding Late Devonian and Permian-Triassic Biotic and Climatic Events (eds. D. J. Over, J. R. Morrow and P. B. Wignall). Toward an Integrated Approach, Develop. Palaeont. Stratigr., **20**: 5–36. Elsevier. Amsterdam.

RACKI G. and BALISŃKI A. (1998) — Late Frasnian Atrypida (Brachiopoda) from Poland and the Frasnian-Famennian biotic crisis. Acta Palaeot. Pol., **43** (2): 273–304.

RACKI G. and HOUSE M. R. eds. (2002) — Late Devonian biotic crisis: ecological, depositional and geochemical records. Palaeogeogr. Palaeoclimat. Palaeoecol., **181** (1–3): 1–374.

REIMOLD W. U., KELLEY S. P., SHERLOCK S. C., HENKEL H. and KOEBERL C. (2005) — Laser argon dating of melt breccias from the

Siljan impact structure, Sweden: Implication for a possible relationship to late Devonian extinction events. Meteor. Planet. Sc., **40** (4): 591–607.

ROHART J. C. (1999) — Palaeozoic rugose corals from central and eastern Iran (A. F. de Lapparent and M. Zahedi collections). Ann. Soc. Géol. Nord, **7**: 47–70.

ROHART J. C. (2000) — Frasnian rugose corals from Chahriseh (Esfahan Province, central Iran). Ann. Soc. Géol. Nord, **8**: 67–71.

RUTTNER A., NABAVI M. H. and ALAVI M. (1965) — Geology of Ozbak-Kuh Mountains (Tabas area, East Iran). Geol. Surv. Iran.

RUTTNER A., NABAVI M. H. and HAJIAN J. (1968) — Geology of Shirgesht area (Tabas area, East Iran). Geol. Surv. Iran, Report, **4**.

SANDBERG C. A. and DREESEN R. (1984) — Late Devonian icriodontid biofacies models and alternate shallow water conodont zonation. In: Conodont Biofacies and Provincialism (ed. D. L. Clark). Geol. Soc. Am. Spec. Pap., **196**: 143–178.

SANDBERG C. A., ZIEGLER W., DREESEN R. and BUTLER J. (1988) — Late Frasnian mass extinction. Conodont event stratigraphy, global changes and possible causes. Courier Forsch.-Inst. Senckenberg, **102**: 263–307.

SANDBERG C. A., MORROW J. D. and ZIEGLER W. (2002) — Late Devonian sea-level changes, catastrophic events, and mass extinctions. Geol. Soc. Am. Spec. Pap., **356**: 473–487.

STÖCKLIN J., EFTEKHAR-NEZHAD J. and HUSHMANDZADEH A. (1965) — Geology of Shotori Range (Tabas area, East Iran). Geol. Sur. Iran, Report, **3**.

STÖCKLIN J. and SETUDEHNIA A. (1991) — Stratigraphic Lexicon of Iran. Geol. Surv. Iran, Report, **18**.

SCHÜLKE I. (1995) — Evolutive prozesse bei *Palmatolepis* in der fruhen Famenne-stufe (Conodonta, Ober-Devon). Göttinger Arbeit. Geol. Paläont., **67**: 1–108.

SCHÜLKE I. (1999) — Conodont multielement reconstructions from the early Famennian (Late Devonian) of the Montagne Noire (southern France). Geol. Palaeont. SB, **3**: 1–123.

TURNER S. (1997) — Sequence of Devonian thelodont scale assemblages in East Gondwana. In: Palaeozoic Sequence Stratigraphy, Biostratigraphy and Biogeography (eds. G. Klapper, M. A. Murphy and J. A. Talent). Studies in Honor of J. Granville ("Jess") Johnson. Geol. Soc. Am. Spec. Pap., **321**: 295–315.

TURNER S., BURROW C. J., GHOLAMALIAN H. and YAZDI M. (2002) — Late Devonian (early Frasnian) microvertebrates and conodonts from the Chahriseh area near Esfahan, Iran. Mem. Ass. Australasian Palaeont., **27**: 149–159.

VALIUKEVICIUS J. J. (1998) — Acanthodian and zonal stratigraphy of Lower and Middle Devonian in east Baltic and Byelorussia. Palaeontographica Abt. A, **248**: 1–53.

VORONTSOVA T. N. (1993) — Rod *Polygnathus sensu lato* (konodonty): fylogeniya i sistematika. Paleont. Zhurnal, **1993** (3): 66–78.

VORONTSOVA T. N. (1996) — Rod *Neopolygnathus* (konodonty): filogeniya i sistematika. Paleont. Zhurnal, **1996** (2): 82–84.

WALLISER O. H. (1966) — Devonian and Carboniferous goniatites in Iran, contribution to the Palaeontology of east Iran. Geol. Surv. Iran, Report, **6**.

WENDT J., KAUFMANN B., BELKA Z., FARSAN N. and KARIMI BAVANDPOUR A. (2002) — Devonian/Lower Carboniferous stratigraphy, facies patterns and palaeogeography of Iran, part I, Southeastern Iran. Acta Geol. Pol., **52** (2): 129–168.

WENDT J., KAUFMANN B., BELKA Z., FARSAN N. and KARIMI BAVANDPOUR A. (2005) — Devonian/Lower Carboniferous stratigraphy, facies patterns and palaeogeography of Iran, part II, Northern and central Iran. Acta Geol. Pol., **55** (1): 31–97.

YAZDI M. (1996) — New age and paleogeographical history redetermination of the Sardar Conglomerate (Tabas, eastern Iran) based on conodont species, comparison of new chronological framework to the age of Upper Paleozoic sediments at Prapotno, Slovenia. Geosc. Quart. J., **5**: 32–41.

YAZDI M. (1999) — Late Devonian-Carboniferous conodonts from eastern Iran. Rivista Italiana Paleont. Strat., **105**: 167–195.

YAZDI M. (2000) — Late Devonian faunal events and sea level changes in east and central Iran. Correlation with global patterns of change. Historical Biology, **15**: 83–89.

YAZDI M., GHOBADI POUR M. and MAWSON R. (2000) — Late Devonian conodonts from the Chahriseh area, central Iran. Records of the Western Australian Museum, Suppl., **58**: 179–189.

YAZDI M., LONG J. A. and TURNER S. (1999) — New placoderm remains from the Late Devonian (Frasnian) of the Shotori Range, eastern Iran. In: Errachidia Meeting IGCP Project 421, April 23, 1999 (eds. R. Feist, J. A. Talent and B. Orth). Abstracts: 45–46.

ZIEGLER W. (1977) — Catalogue of conodonts, **3-E**. Schweizerbart'sche Verlagsbuchhadlung.

ZIEGLER W. and SANDBERG C. A. (1990) — Late Devonian standard conodont zonation. Courier Forsch.-Inst. Senckenberg, **121**.

ZIEGLER W. and SANDBERG C. A. (2000) — Utility of palmatolepids and icriodontids in recognizing Upper Devonian series, stages and possible substage boundaries. Courier Forsch.-Inst. Senckenberg, **225**: 335–437.